AGU ADVANCING EARTH AND SPACE SCIENCES

JGR Oceans

RESEARCH ARTICLE

10.1029/2024JC021211

Tracing Ocean Circulation and Mixing From the Arctic to the Subpolar North Atlantic Using the ^{129}I–^{236}U Dual Tracer

Duncan Dale[1], **Marcus Christl**[2], **Christof Vockenhuber**[2], **Andreas Macrander**[3], **Sólveig Ólafsdóttir**[3], **Rob Middag**[4,5], **and Núria Casacuberta**[1,2]

[1]Department of Environmental Systems Science, ETHZ, Zurich, Switzerland, [2]Laboratory of Ion Beam Physics, ETHZ, Zurich, Switzerland, [3]Marine and Freshwater Research Institute, Hafnarfjörður, Iceland, [4]Royal Netherlands Institute for Sea Research, Texel, The Netherlands, [5]Centre for Isotope Research - Oceans, University of Groningen, Groningen, The Netherlands

Key Points:

- Recirculating Atlantic Water contributes about 40% to Atlantic layer of the East Greenland Current
- Atlantic-origin waters can be traced from the East Greenland Current to the Faroe-Shetland Channel
- Iceland-Scotland Overflow Water and Denmark Strait Overflow Water are traceable separately after joining Deep Western Boundary Current

Supporting Information:

Supporting Information may be found in the online version of this article.

Correspondence to:

D. Dale,
duncan.dale@usys.ethz.ch

Citation:

Dale, D., Christl, M., Vockenhuber, C., Macrander, A., Ólafsdóttir, S., Middag, R., & Casacuberta, N. (2024). Tracing ocean circulation and mixing from the Arctic to the subpolar North Atlantic using the ^{129}I–^{236}U dual tracer. *Journal of Geophysical Research: Oceans*, *129*, e2024JC021211. https://doi.org/10.1029/2024JC021211

Received 15 APR 2024
Accepted 7 JUL 2024

Author Contributions:

Conceptualization: Duncan Dale, Andreas Macrander, Sólveig Ólafsdóttir, Rob Middag, Núria Casacuberta
Data curation: Duncan Dale, Marcus Christl, Christof Vockenhuber, Andreas Macrander, Sólveig Ólafsdóttir, Rob Middag
Formal analysis: Duncan Dale
Funding acquisition: Núria Casacuberta
Investigation: Duncan Dale, Andreas Macrander, Sólveig Ólafsdóttir, Rob Middag, Núria Casacuberta
Methodology: Duncan Dale, Marcus Christl, Núria Casacuberta
Project administration: Duncan Dale, Marcus Christl, Núria Casacuberta

Abstract This study represents the first use of the artificial radionuclides ^{129}I and ^{236}U, released into the ocean mainly from Nuclear Reprocessing Plants, as a dual tracer in the vicinity of Iceland with novel estimation of ocean circulatory pathways and mixing in the region. Iceland lies at the gateway to the Arctic where warm, saline Atlantic waters interact with waters of Arctic origin in ways that have critical consequences for the strength and stability of the Atlantic Meridional Overturning Circulation. Many of these interactions are not yet fully understood, such as how Atlantic water circulates around the Arctic Ocean and Nordic Seas and the composition and fate of the major overflows of the Greenland-Scotland Ridge. Using new and previous measurements of ^{129}I and ^{236}U in seawater, we present a new method of appraising water mass provenance and mixing in the form of the ^{129}I–^{236}U dual mixing plot. With this method, we estimate that at least half the Atlantic-origin water entering the Arctic Ocean circulates around the Canada Basin before exiting at Fram Strait and that this outflow is increased by about 40% by mixing with Return Atlantic Water "short-circuiting" the Arctic Ocean at Fram Strait. We present tracer-based evidence that water carried by the East Greenland Current has an unbroken pathway to the Faroe-Shetland Channel and that Iceland-Scotland Overflow Water (ISOW) entrains 60% Labrador Sea Water during transit past southeast Iceland. We present an unambiguous way to differentiate ISOW from DSOW after they partially merge in the Irminger Sea.

Plain Language Summary This study is the first to use a pair of man-made nuclear products to study ocean currents near Iceland. Understanding these currents is important because Iceland sits where warm Atlantic waters meet colder Arctic waters, affecting a key ocean circulation system and the global climate. However, many details about how these waters move and mix are still unclear. Using new and previous measurements of these tracers in seawater, we demonstrate a new method to estimate the origins of currents and how they mix. We estimate that the outflow of Atlantic-origin water from the Arctic Ocean at Fram Strait is increased by about 40% by Atlantic water bypassing the Arctic Ocean altogether at this location. Some of this Atlantic-origin water then flows all the way from Iceland to Shetland in an unbroken pathway and the water that spills over the Iceland-Scotland ridge increases by 60% by mixing with water from the Labrador Sea southeast of Iceland. Finally, we present a new way to distinguish this Iceland-Scotland Overflow Water from similar water that overflows the ridge at Denmark Strait.

1. Introduction

1.1. Study Area

The Nordic Seas, located between Greenland, Iceland and Norway, are situated at a critical location in the global ocean circulation system (Figure 1) where warm, saline Atlantic waters from the tropics are transported northward to high latitudes releasing heat to the cold sub-arctic atmosphere (Mauritzen et al., 2011). As the warm surface waters cool, become denser and sink, they form deep water masses that eventually overflow the Greenland-Scotland Ridge (GSR). Together with convected waters formed in the Labrador and Irminger Seas, these form the Deep Western Boundary Current (DWBC) and the lower limb of the Atlantic Meridional Overturning Circulation (AMOC) (Frajka-Williams et al., 2019; Lozier, 2023; Weijer et al., 2022). The Nordic Seas are therefore an arena in which ocean circulation dynamics have a critical role in the strength and stability of the AMOC and serve as a major regulator of the redistribution of heat, carbon dioxide and other properties from the ocean surface to the depths, where they may remain partitioned from the atmosphere for hundreds of years. Many key details of

Resources: Duncan Dale, Marcus Christl, Christof Vockenhuber, Andreas Macrander, Sólveig Ólafsdóttir, Rob Middag, Núria Casacuberta
Software: Duncan Dale
Supervision: Núria Casacuberta
Validation: Duncan Dale, Núria Casacuberta
Visualization: Duncan Dale
Writing – original draft: Duncan Dale, Andreas Macrander, Rob Middag, Núria Casacuberta
Writing – review & editing: Duncan Dale, Marcus Christl, Christof Vockenhuber, Andreas Macrander, Sólveig Ólafsdóttir, Rob Middag, Núria Casacuberta

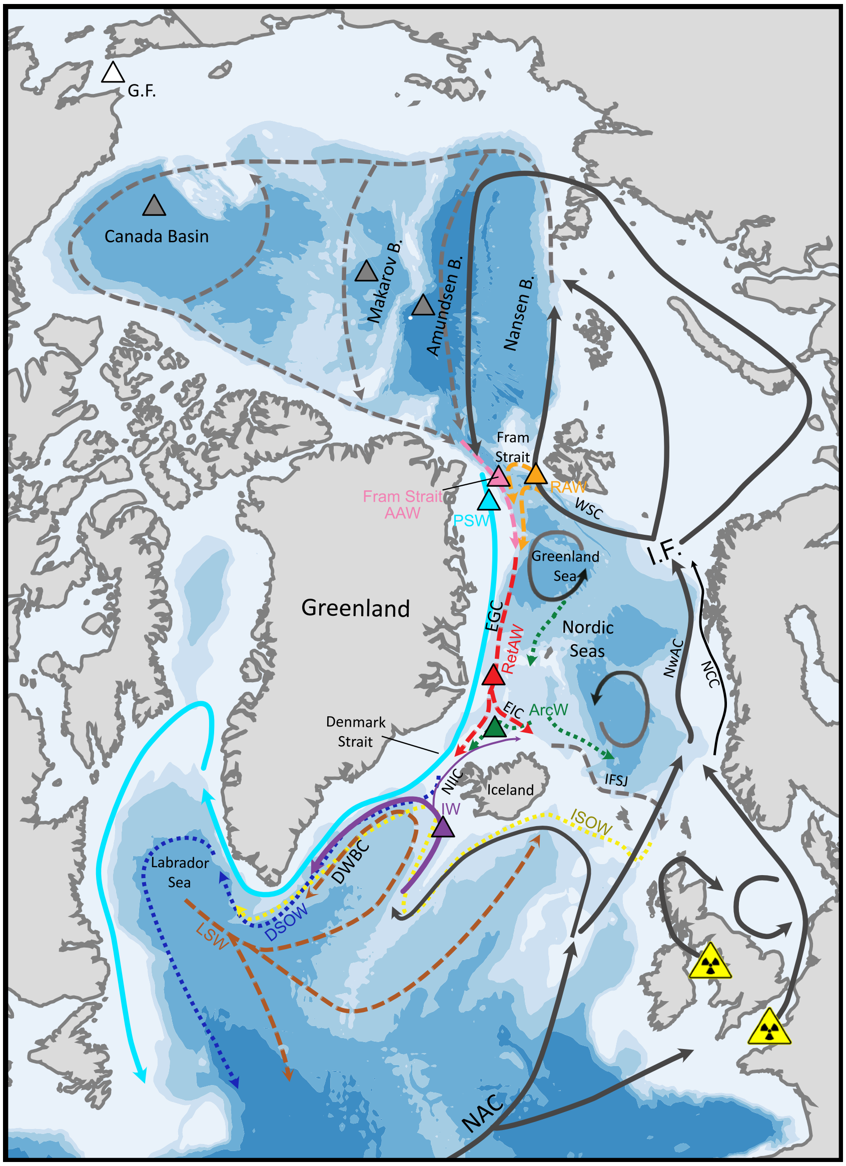

Figure 1. Bathymetric map showing schematic ocean circulation around the Arctic Ocean and Subpolar North Atlantic. Solid arrows represent surface flows, dashed lines are intermediate water masses and dotted lines are deep or bottom flows. Colors represent water masses with a tracer categorization (labeled) as described in Table S2. Triangles in the same color scheme represent approximate ideal locations of endmembers defined in this study. Triangle labeled "G.F." indicates the location of a sample assumed to have a current global fallout tracer signature (Chamizo et al., 2022). Radioactivity symbols indicate the location of Nuclear Reprocessing Plants acting as sources of ^{129}I and ^{236}U to the ocean. "I.F." indicates the location at which input functions of ^{129}I and ^{236}U in surface and Atlantic layers to the Arctic Ocean have previously been defined (see Figure S1 in Supporting Information S1) (Casacuberta et al., 2018; Christl et al., 2015; Smith et al., 2005). Contours represent depth increments of 1,000 m. Acronyms of water masses and currents: ArcW–Arctic-origin Water, DSOW–Denmark Strait Overflow Water, DWBC–Deep Western Boundary Current, EGC–East Greenland Current, EIC–East Iceland Current, Fram Strait AAW–Fram strait Arctic Atlantic Water, IC–Irminger Current, IFSJ–Iceland-Faroe Slope Jet, ISOW–Iceland-Scotland Overflow Water, LSW–Labrador Sea Water, NAC–North Atlantic Current, NCC–Norwegian Coastal Current, NIIC–North Icelandic Irminger Current, NwAC–Norwegian Atlantic Current, PSW–Polar Surface Water, RAW–Recirculating Atlantic Water, RetAW–Return Atlantic Water, WSC–West Spitsbergen Current.

the circulatory regime between the Arctic Ocean and the Subpolar North Atlantic (SPNA) remain incompletely defined despite numerous studies deploying a diverse range of analytical methods. See Table S1 in Supporting Information S1 for a glossary of all acronyms of water masses and currents described in this article.

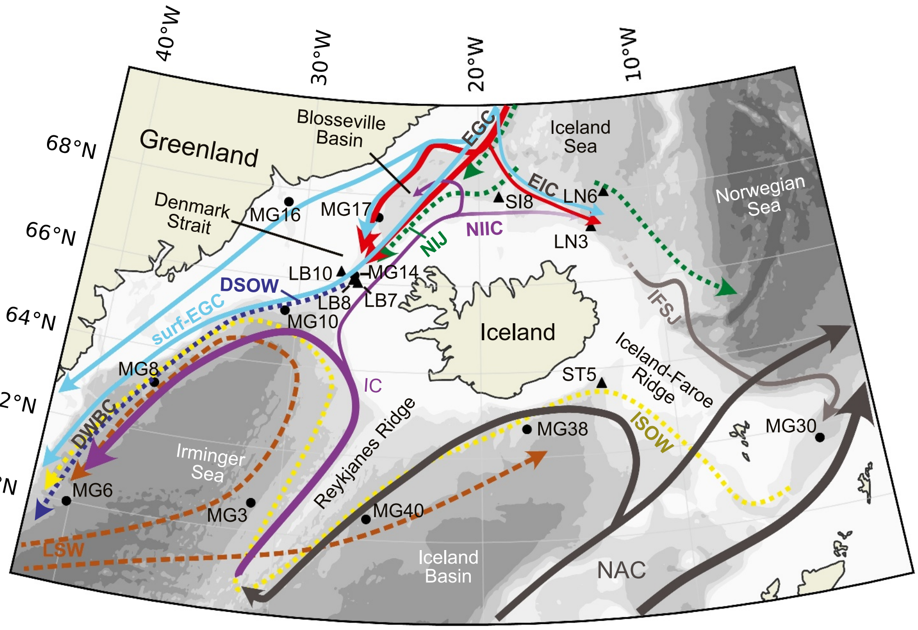

Figure 2. Bathymetric map showing detailed schematic ocean circulation in the Iceland vicinity and locations of stations of samples measured in this study. Arrow formats and colors are as per Figure 1. Contours represent depth increments of 500 m. Acronyms of currents and tracer-categorized water masses: ArcW–Arctic-origin Water, DSOW–Denmark Strait Overflow Water, DWBC–Deep Western Boundary Current, EGC–East Greenland Current, EIC–East Iceland Current, IC–Irminger Current, IFSJ–Iceland-Faroe Slope Jet, ISOW–Iceland-Scotland Overflow Water, LSW–Labrador Sea Water, NAC–North Atlantic Current, NIIC–North Icelandic Irminger Current, NIJ–North Iceland Jet, RetAW–Return Atlantic Water, surf-EGC–surface East Greenland Current.

Atlantic Water in the Arctic Ocean enters via the Barents Sea and Fram Strait before circulating eastward around each of the Arctic basins below the well-stratified halocline. Also entering via the Barents Sea is a layer of low density Polar Surface Water (PSW) formed by cooling of the surface Norwegian Coastal Current (NCC) that circulates along the Russian coast and around Nansen Basin (Rudels et al., 2015). Eventually, the primary exit route from the Arctic Ocean for both layers is at Fram Strait. The Atlantic-origin layer, now referred to in this study as Fram Strait Arctic Atlantic Water (Fram Strait AAW, Figure 1, pink dashed arrow), is joined by a volume of Recirculating Atlantic Water (RAW, orange dashed arrow) that does not circulate around the Arctic Ocean basins but branches westward from the West Spitsbergen Current, effectively short-circuiting the route around the Arctic Ocean (de Steur et al., 2014; Mauritzen et al., 2011; Schaffer et al., 2017). The resulting mixture forming the Atlantic-origin layer of the East Greenland Current (EGC) is often referred to as Return Atlantic Water (RetAW, red dashed arrows) (Harden et al., 2016; Mastropole et al., 2017; Rudels et al., 2005), though due to their similar hydrographic properties it is an unresolved question whether they mix completely during transit to Denmark Strait. Recent estimates of the contribution of RAW to RetAW are not in full agreement. An estimate based on 10 years of mooring data measured an annual contribution varying between 8% and 37% (de Steur et al., 2014) whereas eddy kinetic energy modeling in Fram Strait implies a RAW recirculating fraction varying between 28% and 63% during one modeled year (Hattermann et al., 2016).

The primary conduit of water from the Arctic Ocean to the SPNA, the EGC (see Figure 2 for detailed schematic of circulation around Iceland), is not constituted of water of a single origin but consists of at least two lateral cores (Brakstad et al., 2023; Håvik et al., 2017) carrying a surface layer of PSW (light blue solid arrow) stacked over AAW (becoming RetAW with addition of RAW in Fram Strait) (Rudels, 2002). Below this is a layer of Arctic-origin water (ArcW, green short-dashed arrows) characterized by $\Theta \leq 0°C$ and $\sigma_\theta > 27.97$ kg/m^3 which can be formed in the Arctic Ocean (Rudels et al., 2005) or Nordic Seas (Swift & Aagaard, 1981) and occupies the deep Nordic Seas basins. Circulation of ArcW within and between the Nordic basins is an area of intense recent and ongoing study (e.g., Brakstad et al., 2023) but it has been proposed that the EGC carries with it at least some of the upper layers of ArcW (Rudels, 2002) and that there is some intermixing between the EGC and the ArcW of the

Greenland and Iceland seas, as well as between the constituents of the EGC itself (Håvik et al., 2017; Rudels et al., 2005).

North of Blosseville Basin the EGC branches into two primary cores of a shelf break and separated branch (Harden et al., 2016; Håvik et al., 2017; Våge et al., 2013) with a third core passing eastward to the north of Iceland as the East Iceland Current (EIC) (de Jong et al., 2018; Macrander et al., 2014). Water approaching Denmark Strait from the north is therefore characterized by the three tiers of the EGC: PSW (a) carried above a layer of RetAW (b) below which is the basin-filling ArcW (c). This lower layer is joined by the North Iceland Jet (NIJ), a core of ArcW from the Iceland Sea circulating south along the Iceland shelf at around 650 m depth (Jónsson & Valdimarsson, 2004; Semper et al., 2019). The NIJ has been shown to contribute up to half the volume of Denmark Strait Overflow Water (DSOW, dark blue short-dashed arrow) (Våge, Pickart, Spall, et al., 2011), the rest coming from the denser RetAW and ArcW carried by the EGC, plus some minor subducted PSW (Tanhua, Olsson, & Jeansson, 2005). The specific upstream source of the ArcW carried by the NIJ and the location of the deep convection that is supplying it (e.g., south or northwest Iceland Sea, or the Greenland Sea) are still under investigation (Brakstad et al., 2023; de Jong et al., 2018; Våge et al., 2015). In Denmark Strait, these southward circulating water masses compete for space with northbound Irminger Water (IW, purple solid arrows), mode waters of warm, saline Atlantic Water circulating in the Irminger Basin, with a core in the east of the strait, the North Icelandic Irminger Current (NIIC) (Casanova-Masjoan et al., 2020; Semper et al., 2022).

Overflow of the sill at Denmark Strait by water denser than $\sigma_\theta > 27.8$ kg/m^3, which is typically considered to constitute DSOW (R. R. Dickson & Brown, 1994), is relatively stable at 3.2–3.6 Sv throughout the year (Harden et al., 2016; Jochumsen et al., 2012, 2017; Macrander et al., 2005). This overflow is not continuous in volume but occurs in intermittent boluses of cold, dense water that passes over the deepest section of the ridge at intervals of 2–4 days (Jochumsen et al., 2012; Mastropole et al., 2017). Whilst much progress has been made in characterizing the pathways to the Denmark Strait sill (e.g., Harden et al., 2016; Huang et al., 2019; Lin et al., 2020), the complex dynamics in the strait and mixing with IW in and north of the strait (recirculating purple arrow in Figure 2), make it difficult to estimate which water masses ultimately contribute to DSOW using hydrographic methods alone. Some RetAW in the EGC has been shown to pass over the East Greenland continental shelf and descend into the Irminger Basin further south (Rudels et al., 1999). During its descent along the Greenland shelf edge, DSOW passes IW and Labrador Sea Water (LSW, brown dashed arrows) occupying intermediate depths in the Irminger Basin with concomitant entrainment of these masses into DSOW. Variable estimates have been made for the contribution of each of these main water masses to DSOW, that is, PSW, RetAW, ArcW, IW, and LSW (Harden et al., 2016; Mastropole et al., 2017; Mauritzen, 1996; Rudels, 2002; Tanhua, Olsson, & Jeansson, 2005; Våge, Pickart, Spall, et al., 2011).

The circulation north of Iceland is complex and another area of intense recent and ongoing study. Multiple cores of different origin have been identified, including the westward flowing NIJ and eastward flowing EIC, NIIC, and Iceland Faroe Slope Jet (IFSJ) (Semper et al., 2020). Whilst the downstream pathways of these flows have been relatively well constrained, their origins and their composition are still hotly debated, especially the connectivity between the north of Iceland and DSOW, and with the second major overflow of the GSR: Iceland-Scotland Overflow Water (ISOW, yellow short-dashed arrow). It is not clear, for example, how much of the ArcW arriving at Denmark Strait derives from the EGC, from overturning convection of NIIC water in the south Iceland Sea (Våge, Pickart, Spall, et al., 2011), from deeper convection in the NW Iceland Sea (Harden et al., 2016; Våge et al., 2015), from further north from deep convection in the Greenland Sea (e.g., Brakstad et al., 2023; Huang et al., 2020) or even from the Arctic Ocean (Jeansson et al., 2023). Nor is it clear how much of the ArcW carried by the EGC circulates into the Norwegian Sea via the EIC (de Jong et al., 2018) or is even forced onto the northern Iceland slope to join the NIJ (Rudels, 2022). These unanswered questions are still often represented by question marks on maps of circulation around northern Iceland. Whilst the primary point of overflow of ISOW is the Faroe Bank Channel (FBC), where it is initially termed Faroe Bank Channel Overflow, lesser overflows have been detected at several locations along the Iceland-Faroe Ridge (R. R. Dickson & Brown, 1994; Hansen & Østerhus, 2000). After crossing the Iceland-Faroe-Scotland Ridge, ISOW travels westward in the Iceland Basin following the contour of the Iceland slope and Reykjanes Ridge with a major core passing into the Irminger Basin via the Charlie-Gibbs Fracture Zone (Swift, 1984; Zou et al., 2020). This continues anticlockwise around the Irminger Basin until it reaches the descending DSOW plume southwest of Denmark Strait. Here ISOW begins to circulate between DSOW (below) and LSW (above) as the incipient DWBC (R. R. Dickson & Brown, 1994; Våge, Pickart, Sarafanov, et al., 2011) and the water mass is usually described from this point collectively as

North Atlantic Deep Water (NADW), a water mass that constitutes a large fraction of the deep world ocean (Johnson, 2008) incorporating long-term storage of climatic parameters such as carbon dioxide (CO_2), heat, nutrients, etc.. Their grouping together as a single mass is not only due to their proximity but because of their now very similar hydrographic properties and the difficulty in differentiating the separate original plumes, despite their very different provenances and significance to the composition of the lower limb of the AMOC. Whilst a few hydrographic criteria have been proposed to demarcate them (Tanhua, Olsson, & Jeansson, 2005; B. Dickson et al., 2008), their distinct upstream pathways to southeast Greenland ought to render them clearly identifiable with a suitable upstream transient tracer.

A final important water mass that will be investigated in this work is Labrador Sea Water, an intermediate water formed by wintertime convection in the Labrador and Irminger Seas (Clarke & Gascard, 1983; R. R. Dickson & Brown, 1994). How this water mass interacts with the overflows of the GSR is an open question with important implications for the nature and properties of the lower limb of the AMOC. The volume, depth and hydrographic properties of LSW vary from year to year with some "vintage" years of high production (Yashayaev et al., 2007) making it somewhat problematic to define with a single hydrographic definition, though it is usually easily identified at about 500–2,000 m depth as an oxygen maximum and salinity minimum at about 3–4°C. It occupies this depth in the Irminger Basin and perpetuates eastward around the Reykjanes Ridge via the Subpolar Gyre in approximately 5–7 years to occupy similar depths in the Iceland Basin (Yashayaev & Dickson, 2008). Given this variability, it can be difficult to estimate how much LSW is entrained by the two overflows when they inevitably pass down through the LSW layer, an important question when considering how much of the recently-ventilated LSW is carried into the lower limb of AMOC.

1.2. Artificial Radionuclides ^{129}I and ^{236}U as Tracers of Water Masses

Artificial radionuclides, owing to their unique properties and well-defined anthropogenic sources, have emerged as valuable tracers for investigating oceanic processes. In particular, the long half-life of ^{129}I (15.7 Ma) and ^{236}U (23.4 Ma) along with their conservative behavior (Aldahan et al., 2007; Sakaguchi et al., 2012), high concentration relative to natural sources and well-defined but differing transient release histories into the northeast Atlantic domain (Casacuberta et al., 2018; Christl et al., 2015; Wefing et al., 2021), make them ideal tracers for investigating oceanic transport processes in the Arctic Ocean and SPNA (e.g., Casacuberta & Smith, 2023 and references therein). Recent developments in Accelerator Mass Spectrometry (AMS) have made it possible to measure these radionuclides in concentrations in the order of 1×10^6 at/kg of seawater (Casacuberta et al., 2016) with uncertainties of less than 3% (Christl et al., 2013, 2023; Vockenhuber et al., 2015), which is crucial for distinguishing natural from anthropogenic levels of ^{236}U.

Nuclear Reprocessing Plants (NRP) at La Hague, France, and Sellafield, United Kingdom (radioactive symbols in Figure 1), have been releasing anthropogenic radionuclides since the 1950s, injecting substantial quantities of ^{129}I and ^{236}U into the seas around the British Isles (Christl et al., 2015; He et al., 2013). These mix in the North Sea (Figure 1) before being transported north to the Arctic Ocean via the NCC, effectively providing a point-like transient source of these tracers to the Arctic region (Christl et al., 2015, 2017; Edmonds et al., 2001; Smith et al., 2011). This transient signature combines with a global fallout signature of ^{236}U to the surface oceans from atmospheric nuclear bomb tests in the 1950 and 1960s (Christl et al., 2015; Snyder et al., 2010). The resulting total release to the ocean in the vicinity of the British Isles represents a concentration of ^{129}I four orders of magnitude greater than the 1–2 $\times 10^7$ at/kg found in seawater affected by natural background levels (Snyder et al., 2010) and a ^{236}U signal one order of magnitude greater than seawater with a global fallout concentration of about 6×10^6 at/kg such as currently found in the surface Pacific Ocean (Chamizo et al., 2022). This high concentration relative to global fallout and natural background concentrations delivers a high sensitivity that makes these radionuclides powerful tracers of ocean circulation downstream of the input around the British Isles. Previous research has successfully defined input functions for these two tracers in the surface and mid-depth layers entering the Arctic Ocean (see Figure S1 in Supporting Information S1) (Wefing et al., 2021). It has demonstrated that, when used together as a dual tracer, they offer valuable insights into Arctic Ocean circulation dynamics and timescales.

This study explores the potential of the ^{129}I - ^{236}U dual tracer in revealing details of ocean circulation between the Arctic Ocean and the Nordic Seas and their southern outflows. Using new tracer data measured in the vicinity of Iceland and the wider SPNA, combined with a reanalysis of previous measurements made in the Arctic Ocean and at Fram Strait, we demonstrate the potential of the dual tracer to address some of the open questions in the Arctic-

SPNA domain. In this paper, specific questions will be addressed: (a) how much Atlantic-origin water circulates around each of the Arctic basins or even short-circuits the Arctic Ocean altogether by recirculating south at Fram Strait; (b) how much do the water masses carried by the EGC mix with adjacent masses between Fram and Denmark Straits; (c) which water masses contribute to the two main overflows, DSOW and ISOW; and (d) can the tracers be used to quantify the downstream mixing of the overflows and provide an improved method of differentiating them from each other after they join the incipient DWBC?

By measuring the downstream progress of the dual tracer in the seas around Iceland, we establish new endmember values for key water masses in the region for use in this and future studies. Ultimately, we show it is possible to characterize circulation pathways in this domain and estimate mixing of water masses using the $^{129}I - ^{236}U$ dual tracer. An overarching goal of this study is to investigate if the techniques used can compliment or even improve upon more traditional physical oceanographic methods deployed to address similar questions.

2. Methods

2.1. Sampling

Samples measured for this study were collected during two oceanographic cruises in 2021, referred to as "Iceland21" and "MetalGate" (see dots and triangles in Figure 2). Iceland21 samples ($n = 45$) were collected in February 2021 during routine monitoring by the Marine and Freshwater Research Institute (MFRI) of Iceland on *R/V Bjarni Sæmundsson*. MetalGate samples ($n = 98$) were collected in August 2021 on board *R/V Pelagia* during the MetalGate cruise, part of the international GEOTRACES program and operated by the Royal Netherlands Institute for Sea Research (NIOZ). During both cruises, seawater was retrieved from Niskin bottles mounted on a conductivity-temperature-depth (CTD) rosette. Samples were collected in 5 L (Iceland21) and 3 L (MetalGate) Nalgene Cubitainers after two initial rinses of seawater from the respective Niskin bottle and no further treatment. Samples were shipped to ETH Zurich where ≈200 mL aliquots were separated for ^{129}I analysis, the remainder to be used for the ^{236}U measurement.

In addition to samples measured in this study, we re-evaluate a number of published sample sets collected on previous expeditions in the Arctic Ocean in 2015 (Casacuberta et al., 2018; Chamizo et al., 2022) and Fram Strait in 2016 (Wefing et al., 2019) as potential inputs to the Nordic Seas and SPNA. All samples analyzed in this study along with their basic hydrographic properties are listed in Table S3.

2.2. Sample Processing and Measurement

Each ≈200 mL sample was processed to separate and purify iodine before measurement of ^{129}I concentration following the method described by Wefing (2021). All processed samples were measured at the Laboratory of Ion-beam Physics (LIP) at ETH Zurich using the 0.5 MV Accelerator Mass Spectrometry (AMS) system: TANDY. Reproducibility was assessed based on repeat measurements of an in-house standard (a large volume of seawater collected from a single Niskin bottle on a previous expedition in the northeast Atlantic Ocean in 2021) purified at the same time as samples. This resulted in an average concentration with a 1 standard deviation of 4% that was applied as uncertainty of the final ^{129}I concentration values.

Seawater samples for the measurement of uranium isotopes were spiked with 1pg ^{233}U, preconcentrated, purified by ion exchange chromatography using UTEVA® (Triskem International) resin columns, oxidized and pressed into AMS targets in the method described by Wefing (2021). Samples were measured as $^{233}U/^{238}U$ and $^{236}U/^{238}U$ at LIP on the 300 kV Multi-Isotope Low Energy AMS (MILEA) system using in-house standard "ZUTRI" using correction procedures as outlined in Christl et al. (2023). Concentrations of both ^{236}U and ^{238}U were calculated from the measured concentration of the ^{233}U spike, including an uncertainty for the added quantity of spike. Analytical uncertainties of 1.9%–5.0% of 1 standard deviation (1-σ) were obtained for >99% of samples.

2.3. Water Mass Classification

We have created a framework of water mass classification based on several published sets of water mass definitions into which we assign samples measured or analyzed in this study (Table S2). Characterizing water masses with definitions based on hydrographic properties across a large area can be problematic. Different studies may use different water mass names that may only partially correspond with those in other studies with different purposes or region of study. Additionally, a water mass definition based on properties at the source region of a mass, such as salinity and temperature, will inevitably become less appropriate with distance from the source region, or may be changing with time. This study does not seek to reproduce studies of ocean circulation in the Arctic Ocean and SPNA based on hydrographic properties but to derive unique conclusions from the concentrations of the two tracers ^{129}I and ^{236}U in broadly defined water masses. The classification used is based primarily on the general upstream zone of origin of each mass as outlined in Table S2. In this manner, we are able to attribute samples to currently understood major water masses and circulation architecture whilst allowing the tracers to provide novel insights into the circulation pathways and mixing in the Arctic Ocean and SPNA.

The Θ-S properties of all measured stations relative to previously defined water masses are shown in Figure 3 with separate plots for the general areas NW, NE, SW and SE of Iceland; zones in which Θ-S profiles are similar and comparable.

To the north and west of Iceland (Figure 3a), sampled stations are generally characterized by PSW over RetAW (AAW or DAAW) with station MG14 reaching down to the top of the ArcW layer (AIW, ISDW or NSDW). All stations except MG17 also pass through a layer of IW penetrating from the south. Within this upper IW layer are some cold, fresh Θ-S-excursions representing interleaving of shallowly-convected PSW with RetAW or IW.

To the north and east of Iceland (Figure 3b), stations LN3 and LN6 are deep enough to encounter Iceland Sea Deep Water (ISDW) ($\sigma_{0.5}$ > 30.444 kg/m^3), which is ArcW characteristic of the Iceland Sea Basin (Jeansson et al., 2008, 2023; Rudels et al., 2005). The upper column of the three stations close to Iceland (SI8, LN3, LN6) is occupied by RetAW. There are again indications of interleaving of PSW with RetAW in the upper column in the form of cold, fresh excursions. The base of station MG30 in the Faroe-Shetland Channel indicates Norwegian Sea Deep Water (NSDW) with overlying Norwegian Sea Arctic Intermediate Water (NSAIW) (Jeansson et al., 2023), both classified as ArcW in this study. Whereas this deep portion of station MG30 (where $\Theta < 0.25$°C) matches the characteristics of the other three stations north of Iceland, the upper column of station MG30 records Θ-S characteristics of Modified East Icelandic Water (MEIW) capped with Modified North Atlantic Water ((MN)AW) (Hátún et al., 2021; Read & Pollard, 1992), which suggest origins from north of Iceland and the North Atlantic Current (NAC), respectively.

Southwest of Iceland (Figure 3c), the bottom of stations MG6, MG8 and MG10 have Θ-S properties close to the definition of DSOW proposed by Liu and Tanhua (2021) (not shown) whereas station MG3 has its base very close to the definition of ISOW according to the same authors. The profiles of stations MG6, MG8 and MG10 all indicate that ISOW is present above DSOW in the water column at these three locations using the $\Theta = 2$°C isotherm to differentiate these overflow waters as proposed by Tanhua, Olsson, and Jeansson (2005), although at MG10 the layer above DSOW is a borderline mixture of ISOW and LSW. All stations then pass upward through LSW with swiftly oscillating Θ-S curves implying significant interleaving of LSW with 7°C Subpolar Mode Water (SPMW7) or Irminger Subpolar Mode Water (IrSPMW). These are mode waters formed from the air-sea cooling of Atlantic Water of the NAC as it circulates north and westward around the subpolar gyre to produce progressively cooler and fresher mode waters such as the SPMW7 found just east of the Reykjanes Ridge and IrSPMW found in the Irminger Sea (Brambilla et al., 2008; García-Ibáñez et al., 2018; Thierry et al., 2008). All stations recorded surface mixed layers with $\Theta \approx 9$–10°C.

Figure 3d includes station Θ-S-profiles to the south and east of Iceland. Stations ST5, MG38 and MG40 present at their bases water typical of ISOW in the eastern North Atlantic (García-Ibáñez et al., 2018). Of these three stations, MG38 and MG40 show salinity minima characteristic of LSW, though somewhat mixed with IrSPMW/SPMW7. There is no indication of LSW at station ST5. The upper column of all three stations is dominated by IrSPMW, SPMW7 or SPMW8 capped with surface/mixed waters up to ∼12.5°C.

2.4. Binary Mixing Model

The main tool used in this paper to estimate mixing of water masses is the dual tracer mixing plot (Figure 4). By plotting the ^{129}I and ^{236}U concentrations of seawater samples that have been attributed to specific water masses using hydrographic properties we are able to make inferences about water mass provenance and mixing. Whilst the tracer signature of the Atlantic water entering the Arctic Ocean is changing over time (green crosses), the rate of change of the inputs is slow enough that we can compare measurements of water masses relatively proximal in

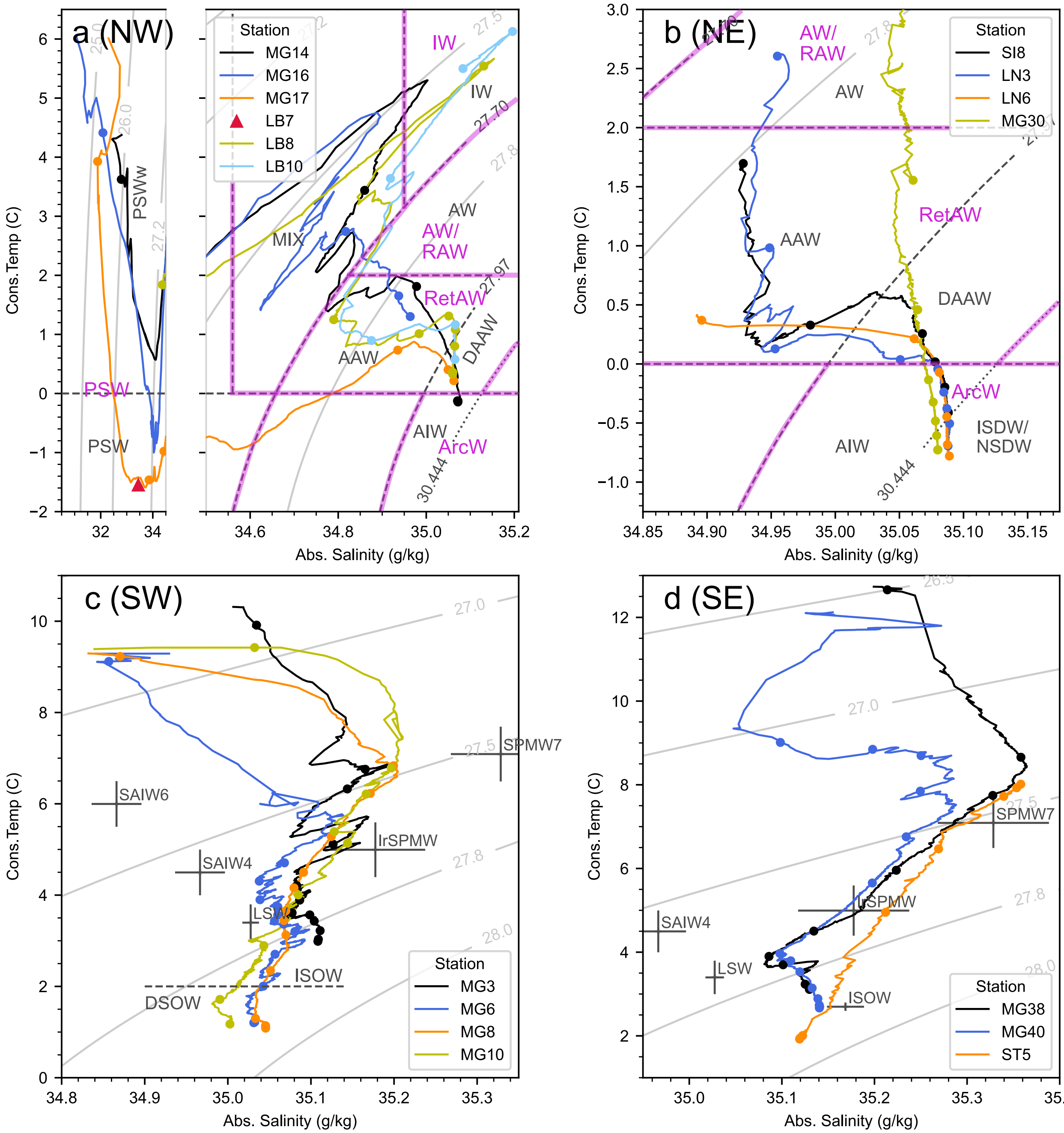

Figure 3. Plot of Θ-S properties of stations sampled in this study grouped by areas NW (a), NE (b), SW (c), and SE (d) of Iceland. Locations of stations given in Figure 2. Circles indicate position of samples measured in this study. Solid and dotted gray contours are σ_0 and $\sigma_{0.5}$ isopycnals, respectively. Dashed lines in (a) and (b) indicate divisions between water masses as defined by Rudels et al. (2005). Magenta lines and labeled areas represent tracer seawater categories as defined in this study (refer to Table S2 for key of categories). Cross markers in (c) and (d) represent source water type (SWT) definitions in the North Atlantic (±1-σ) as per García-Ibáñez et al. (2018). Dashed line in (c) represents $\Theta = 2°C$ proposed demarkation between ISOW and DSOW as per Tanhua, Olsson, and Jeansson (2005). Water mass acronyms: AAW–Arctic Atlantic Water, AW–Atlantic Water, AIW–Arctic Intermediate Water, DAAW–Dense Arctic Atlantic Water, DSOW–Denmark Strait Overflow Water, IrSPMW–Irminger Subpolar Mode Water, ISOW–Iceland-Scotland Overflow Water, LSW–Labrador Sea Water, MIX–Mixed layer, NDW–Nordic Seas Deep Water, PSW–Polar Surface Water, PSWw–warm Polar Surface Water, SAIW4–Subarctic Intermediate Water 4°C, SAIW6–Subarctic Intermediate Water 6°C, SPMW7–Subpolar Mode Water 7°C.

the ocean circulatory system taken within a few years whilst neglecting the change in the inputs. In this manner, a pseudo steady-state snapshot of a region such as the Nordic Seas can be studied on a mixing plot as if it represents one point in time.

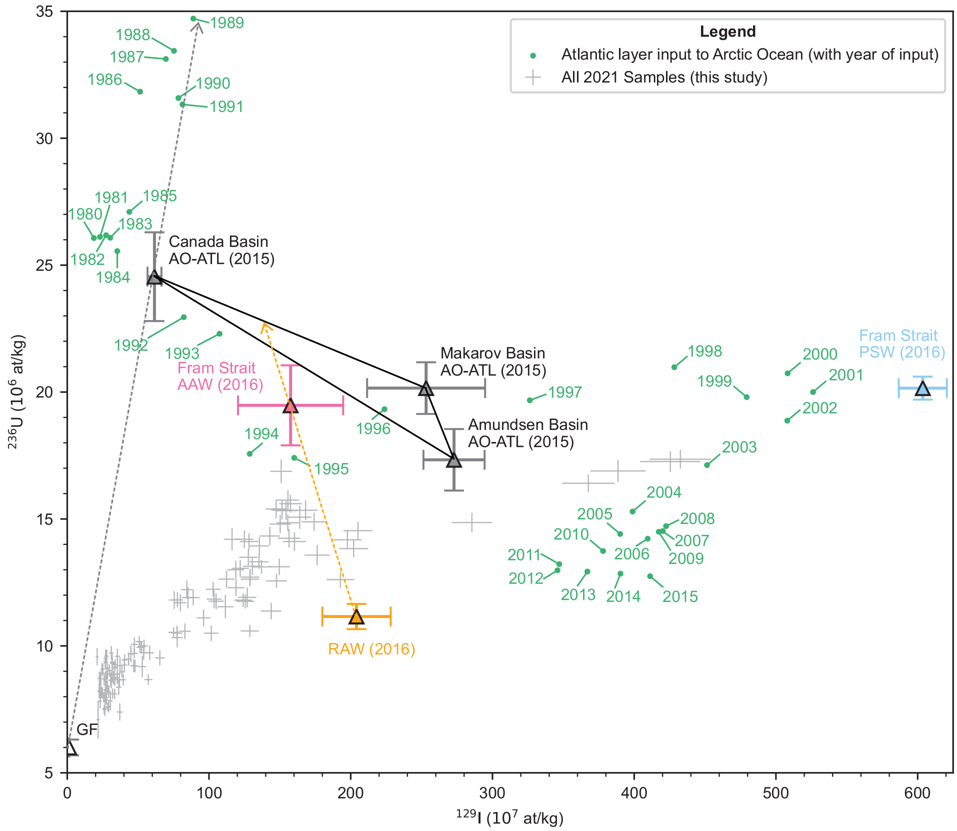

Figure 4. ^{129}I–^{236}U mixing plot highlighting endmembers of water masses found in the Arctic Ocean and at Fram Strait. Triangles represent endmembers of water masses defined as per data in Table S2. Colors correspond with colors of water masses as depicted in Figures 1 and 2. Error ticks represent 1-σ of values of samples used to define endmembers. Gray cross markers are all samples measured in this study including analytical uncertainty. Green dots indicate the tracer signature of each year of Atlantic layer input of ^{129}I and ^{236}U to the Arctic Ocean (at location marked "I.F." on Figure 1) as per Casacuberta et al. (2018). Triangle labeled "GF" in lower left corner indicates an endmember of seawater assumed to have a current global fallout concentration (Chamizo et al., 2022). Black solid lines define tracer space expected to be occupied by any product of mixing of Atlantic-origin water from the three Arctic Ocean basins (AO-ATL, see Table S2 for hydrographic selection criteria). Orange dashed arrow signifies removal of effect of any dilution of Fram Strait AAW by RAW. Gray dashed arrow represents removal of effect of dilution of Canada Basin AO-ATL (as measured in 2015) with water carrying a global fallout tracer signature.

A key component of the dual mixing plot is endmembers: the tracer signature of a water mass in a specific location that is a potential input to an area under study. In this study, we use previously published data from the Arctic Ocean and Fram Strait as inputs to the western Nordic Seas. Six such input endmembers are depicted in Figure 4 and the samples and locations used to define them are listed in Table S3 and Figure 1, respectively. The Fram Strait PSW represents the input of surface waters to the Nordic Seas via the surface EGC (0–25 m depth), the other endmembers except "GF" represent waters of Atlantic origin (AO-ATL) circulating at about 250–900 m depth. The "GF" endmember (^{129}I = 1.3 × 10^{7} at/kg, ^{236}U = 6.0 × 10^{6} at/kg) represents water with a global fallout signature as measured in the Bering Strait in 2015 (Chamizo et al., 2022). Similar surface values have also been observed in the northeast Atlantic Ocean (^{129}I = 5 × 10^{7} at/kg) (He et al., 2013) and central Atlantic Ocean (^{236}U = 5.7 × 10^{6} at/kg) (Casacuberta et al., 2014). Values representing the Atlantic layer input function to the Arctic Ocean (Casacuberta et al., 2018; Wefing, 2021) have been plotted to provide an indication of the changing signature of the dual tracer in Atlantic-origin water entering the Arctic Ocean over a timescale of years and decades.

The principle of the dual mixing plot is that if a water mass is formed by the mixing of two input water masses, assuming conservative tracer behavior and by simple mass balance, the product mass must have a tracer signature that plots on the line between that of the two inputs. Moreover, the location along the line will indicate the relative mixing proportions of the two endmembers. The closer a product water mass plots to an input endmember, the more of that input constitutes the product water mass in linear proportion to the line distance. Similarly, if three endmembers mix to produce a new water mass, the product will plot in the triangle made by the three inputs with the location within the triangle indicating the constituent proportions. If a product water mass plots outside the space defined by input endmembers, one or more additional water masses must be involved in producing the final water mass. This (or these) other input(s) must have a tracer signature that "pulls" the product mass signature in the relevant direction in tracer space. In the example of Figure 4, Fram Strait AAW does not fall in the triangle of the three AO-ATL inputs via the three Arctic Ocean basins as it has been "pulled" toward the RAW endmember by early mixing with that water mass north of Fram Strait. By projecting away from RAW (orange dashed line), we can remove the influence of the mixing with RAW and estimate the relative proportion of Canada Basin AO-ATL versus Makarov and Amundsen Basins from where the dashed line intercepts the lines between the basin endmembers. See Section 4.1 for further details.

3. Results

3.1. Tracer Distribution

The results of all ^{129}I and ^{236}U measurements in this study are shown in Table S3. The concentration of ^{129}I in seawater is presented in units of 10^7 atoms per kg of seawater (10^7 at/kg). The contribution of ^{129}I from bomb tests in the mid-twentieth century is expected to be almost negligible ($\sim$1–2 $\times$ 10^7 at/kg) and natural lithogenic background is not expected to measure above the bomb spike (Raisbeck & Yiou, 1999). Values measured in this study vary from (21.1 $\pm$ 1.1) $\times$ 10^7 at/kg in IW in the Irminger and Iceland Basins to (433 $\pm$ 22) $\times$ 10^7 at/kg in the PSW north of Denmark Strait (station MG17). Concentrations of ^{236}U in seawater are presented in units of 10^6 at/kg. Waters that have had contact with the surface ocean since the peak bomb spike in the 1960s are expected to have a residual global fallout concentration of ~6 $\times$ 10^6 at/kg (Chamizo et al., 2022) with negligible contribution from lithogenic background (Steier et al., 2008). Concentrations measured in this study range from (7.1 $\pm$ 0.8) $\times$ 10^6 at/kg in ArcW (ISDW) and (7.4 $\pm$ 0.2) $\times$ 10^6 at/kg in IW south of Iceland up to (17.4 $\pm$ 0.4) $\times$ 10^6 at/kg in the PSW north of Denmark Strait. It should therefore be noted that the range of seawater ^{236}U concentrations in the study area are only 1.2 to 3 times the global fallout value compared with three orders of magnitude variation in ^{129}I concentrations above global fallout.

The distribution of tracer concentrations in Θ-S-space north and south of Iceland is shown in Figure 5. North of Iceland (Figures 5a and 5b), ^{129}I and ^{236}U have their highest concentrations in PSW and show moderate to high in RetAW (AAW and DAAW), indicative of the direct (albeit circuitous) pathways to these water masses from the NRP source region. The lowest concentrations are seen in IW from south of the GSR and in the deep, cold and dense waters of the Nordic Seas basins indicative of the low recent connectivity of these water masses with the Nuclear Reprocessing Plant (NRP) tracer source waters.

South of Iceland (Figures 5c and 5d), the concentration of ^{129}I is generally lower than to the north (hence the reduced scale in Figure 5c). However, it can still clearly be observed that the highest ^{129}I and ^{236}U concentrations are in the deep, dense waters of the overflows (DSOW and ISOW) and, to a lesser extent, in LSW. The distribution of ^{236}U in the mode waters south of Iceland is on the low side and somewhat difficult to distinguish from the expected current global fallout value of ~6 $\times$ 10^6 at/kg. These mode waters are less well differentiated by the ^{129}I concentrations compared with the ^{236}U concentrations, which is remarkable given the larger variance overall in ^{129}I compared to ^{236}U. However, it should still be noted that ^{129}I concentrations in the mode waters are still 10–20 times higher than expected for waters untouched by NRP releases.

Station profiles of all tracer measurements made in this study are shown in Figure 6 arranged in quadrants around Iceland as per Figure 3. The tracer category of the dominant water masses at all depths as defined by the categorization scheme outlines in Table S2 is labeled for each quadrant. Northwest of Iceland (Figure 6a), that is, in or just to the north of Denmark Strait, the tracer profiles for all stations can be considered at three depth ranges. The highest tracer values for both tracers in the entire study are found here in the surface layer down to $\sim$100 m which, as outlined above, represents PSW carried as the surface layer of the EGC. Below this is a layer at about 100–250 m with generally lower concentrations of both tracers with the exception of station MG17, which is 150 km NE of Denmark Strait. Reference to Figure 3a shows this layer in Denmark Strait to be dominated by IW which, from the profile of both tracers at station MG16, appears to extend westward onto the east Greenland shelf. Below 250 m, both tracer concentrations generally converge to a higher and narrower range for all stations. There is

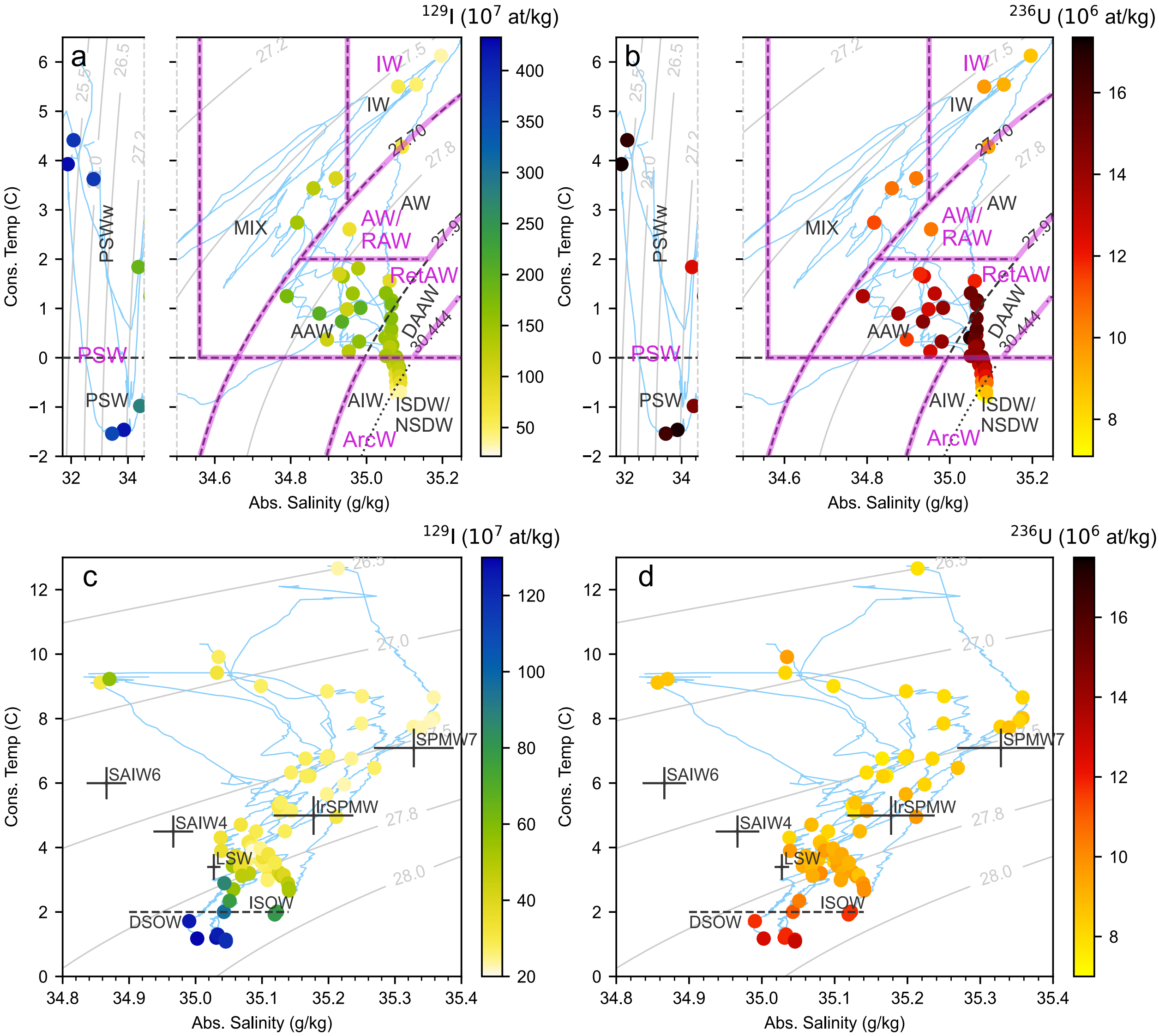

Figure 5. Θ-S plots of all stations sampled in this study to the north (a), (b) and south (c), (d) of the GSR showing measured concentration of ^{129}I (a), (c) and ^{236}U (b), (d). Contours and water mass definitions are as per Figure 3. Blue lines are station Θ-S profiles as per Figure 3. Note reduced ^{129}I scale in (c).

notable variation in tracer profiles at this level, both between stations and between tracers for each station, implying a rather complex mixing regime for the various water masses converging at Denmark Strait. ^{236}U concentrations below 250 m are at some stations almost as high as at the surface. All samples below 250 m have Θ-S properties of RetAW except for station MG14, the lowest three samples of which indicate ArcW.

North and northeast of Iceland (Figure 6b), the tracer profiles of both tracers are remarkably similar between stations, except for the top 400 m of station MG30. The upper column of MG30 is occupied by Modified North Atlantic Water (MN)AW from south of the GSR as characterized by Hátún et al. (2021) and surface tracer values converge with the low values seen in the upper column south of the ridge (Figure 6c). At the surface of the other three stations (SI8, LN3, LN6), the lower tracer values correspond with the mixed layer and variable proportions of SAIW and PSW interleaving with the RetAW below. All four station profiles show peaks in ^{129}I and ^{236}U at ∼400–600 m depth, which notably corresponds with the RetAW measured in the EGC (Figure 6a). Below the RetAW peak, ^{129}I and ^{236}U concentrations decrease smoothly and continuously with depth at all four stations with increasing predominance of ArcW water. The lowest tracer concentrations are found in ISDW and NSDW at the base of stations LN3, LN6 and MG30, with the lowest ^{236}U concentration of the entire study area found at 1,855 m at station LN6.

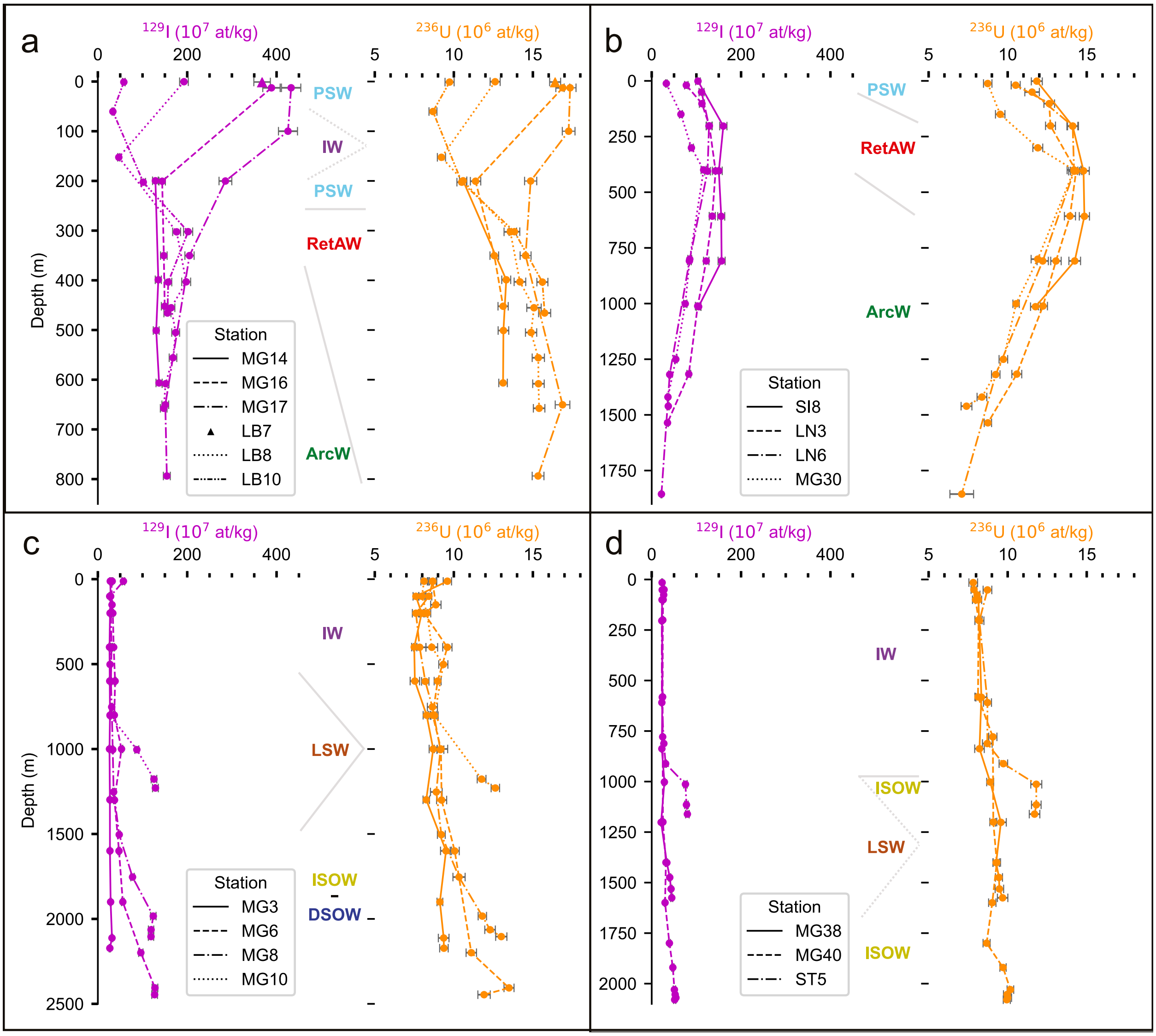

Figure 6. Station profiles of ^{129}I and ^{236}U grouped by stations to the NW (a), NE (b), SW (c), and SE (d) of Iceland as per Figure 3. Labels in the center of each plot indicate the dominant water mass found at each depth categorized by seawater tracer category as per Table S2. Solid lines in the center indicate the approximate boundary between water masses and dotted lines indicate where a water mass is only sometimes present at one or more stations at the depths indicated. For reference, global fallout concentrations at locations not influenced by NRPs are 1.3×10^7 at/kg for ^{129}I and 6.0×10^6 at/kg for ^{236}U (Chamizo et al., 2022).

Southwest of Iceland in the Irminger Sea (Figure 6c), there is almost no sign of the elevated tracer values seen in the PSW in Denmark Strait. This and the Θ-S profiles of Figure 3c indicate that none of these stations intersected PSW of the surface-EGC. It is also immediately obvious that the elevated tracer signatures that are present at 250–800 m depth close to the sill in Denmark Strait (LB8, LB10, MG14) are not present at the same depth at any stations south of the strait. This is despite at least one sample of RetAW in Denmark Strait (station LB8, 302 m depth) having a potential density anomaly $\sigma_\theta = 27.73$ kg/m^3, less dense than the putative cutoff for water dense enough to join overflow waters (R. R. Dickson & Brown, 1994). All four stations in Figure 3c indicate the presence of a layer influenced by LSW and stations MG6, MG8, and MG3 suggest the presence of ISOW although it is not obvious from Figure 6c if these water masses exhibit a distinctive tracer signature. The most distinctive feature of Figure 6c are the peaks in both tracers at the base of stations MG6, MG8, and MG10 where Θ-S properties indicate the presence of DSOW. The peaks are particularly pronounced for ^{129}I, concentrations of which are four to five times those of the upper column at these locations.

Tracer profiles of stations to the southeast of Iceland (Figure 6d) are very similar to those in the Irminger Sea (Figure 6c) with flat upper columns over more modest peaks at the bases. Salinity minima indicate the presence of LSW at intermediate depths (Figure 3d), especially in the western Iceland Basin at station MG40. Whilst it is not clear from Figure 6, reference to Table S1 in Supporting Information S1 shows that the presence of LSW corresponds with a slight elevation in both tracers at these depths, most notably ^{236}U concentration. At the base of these three stations, particularly station ST5, there is a clear peak in both tracers where Θ-S properties match that of ISOW.

4. Discussion

4.1. Mixing of Atlantic-Origin Water in the Arctic Ocean and Fram Strait

In order to assess the potential of the ^{129}I - ^{236}U dual tracer to estimate mixing within and between Atlantic and Arctic origin water masses in the Arctic-SPNA domain, we use the binary mixing plot, described in Section 2.4 (Figure 4). First, we assess the relative mixing in Fram Strait of Atlantic-origin water (AO-ATL), which is an endmember that results from a mixture of the Atlantic waters that circulated through different Arctic basins (see Figure 1 for circulation features and location of endmembers). At Fram Strait, AO-ATL comes together to form the Atlantic-origin component of the incipient EGC, here called Fram Strait AAW (Figure 4, pink triangle). A water mass formed by the mixing of AO-ATL from the Canada, Makarov and Amundsen basins (gray triangles) should plot in the area defined by these three endmembers. Whilst the 1-σ area of the Fram Strait AAW endmember (pink ticks) does slightly overlap this triangle, the mean value is noticeably below it. This suggests that the Fram Strait AAW endmember has been mixed with one or more water masses other than the three AO-ATL endmembers. The most feasible candidate is some pre-mixing with RAW (orange triangle) upstream of Fram Strait, though it is difficult to distinguish these two Atlantic-origin water masses at this location using only Θ-S properties once they begin mixing (Håvik et al., 2017). We can remove the influence of this RAW input by projecting in a straight line (orange dashed) away from that endmember back to the triangular space defined by the three AO-ATL endmembers. With or without this adjustment, it can be seen that the mixing plot indicates that at least half of the Fram Strait AAW comes from Atlantic waters that have circulated through the Canada Basin.

Whilst this is a demonstration of the ability of the mixing plot to infer mixing proportions, in this instance the three input endmembers in the Arctic Ocean are rather far upstream from Fram Strait for the calculation to be reliable given the transient nature of the tracer input functions and the uncertain transit times of AO-ATL from each of the basins to Fram Strait. In particular, the transit time between the location of measurement in the Canada Basin to Fram Strait is not known and the actual endmember value contributing to Fram Strait AAW during the measurement year of 2016 might actually represent several years prior to the Canada Basin AO-ATL 2015 value plotted in Figure 4. Reference to the Atlantic layer input function (green dots) shows that, allowing for dilution with water with a global fallout tracer signature (gray dashed line), the Canada Basin AO-ATL 2015 endmember was carrying a tracer signature of Atlantic water that entered the Arctic Ocean (location marked "I.F." on Figure 1) around 1990. A transit time from Canada Basin to Fram Strait of even 10 years would only shift the Canada Basin AO-ATL endmember marginally to the left in the plot (to the line joining "GF" and 1980 green dot). However, applying the same treatment to the Makarov and Amundsen Basin AO-ATL endmembers, which indicate Atlantic water of input years 1996 and 1997, respectively, even 1–3 years transit time between those basins and Fram Strait would shift their locations on Figure 4 dramatically to the left in accounting for this transit time. The assessment of at least 50% of Fram Strait AAW coming from Canada Basin is therefore only rigorously valid when treating Figure 4 as a steady-state model and this represents a limitation of this method where sampled water masses are particularly far apart in location and transit time between locations. However, the method is more robust in the studied area as sampled water masses are closer together, spatially and temporarily, as is the case with mixing in and south of Fram Strait.

4.2. Mixing of Recirculating Atlantic Water With the East Greenland Current

This assessment of mixing at Fram Strait can also be applied to the mixing of RAW with Fram Strait AAW and thereby estimate the contribution of RAW to the RetAW carried by the EGC to Denmark Strait. Estimating the contribution of RAW to RetAW by traditional hydrographic methods, such as flow velocity moorings (de Steur et al., 2014) or eddy kinetic energy modeling (Hattermann et al., 2016), are complicated by the highly turbulent and variable flow dynamics in Fram Strait and the overlapping Θ-S properties of the water masses involved

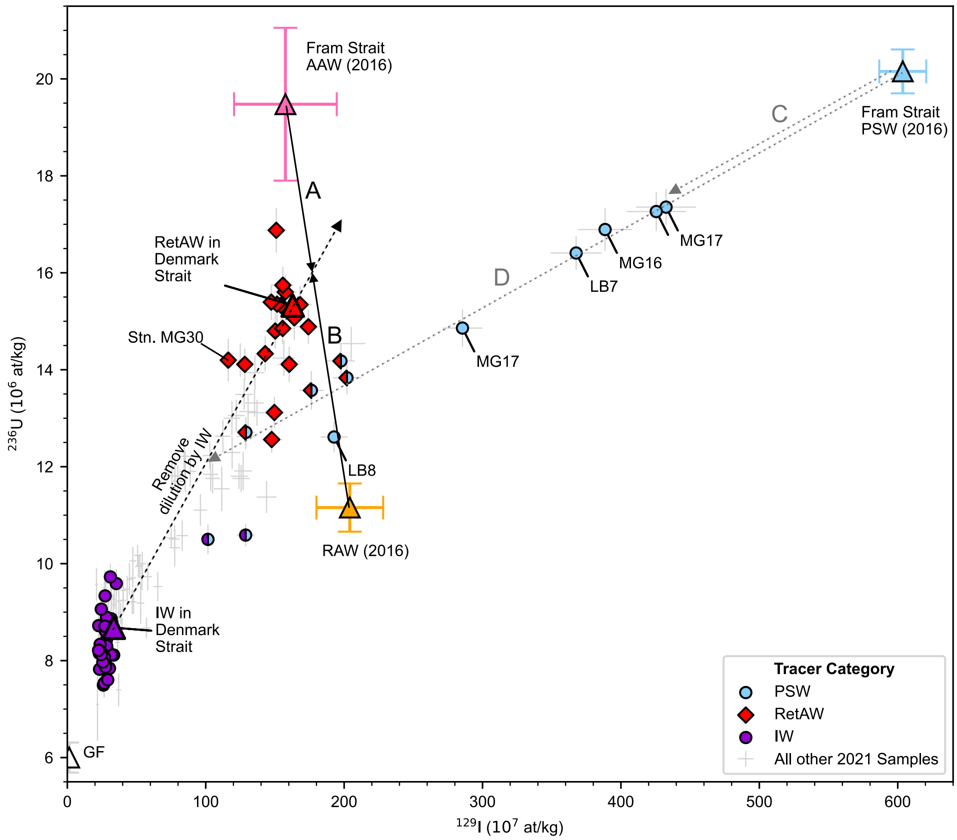

Figure 7. ^{129}I–^{236}U mixing plot showing PSW and Atlantic-origin waters and their mixing north of the GSR. Triangles with error ticks represent endmembers of water masses defined as per data in Table S2. Colored markers correspond to samples of Polar Surface Water (PSW), Return Atlantic Water (RetAW) and Irminger Water (IW) measured in this study. Labeled triangles are endmembers of RetAW and IW defined from samples in this study. All colors correspond with colors of water masses as depicted in Figures 1 and 2. Half-and-half markers represent samples with clear evidence from Θ-S properties of mixing of the two relevant water masses. Dashed line represents removal of effect of IW in Denmark Strait mixing with RetAW. Solid arrows indicate expected tracer value of mixing of RAW with Fram Strait AAW before any dilution with IW. Contribution of RAW to RetAW (fraction) = length A/(A + B). Dotted lines represent dilution of Fram Strait PSW with IW and RetAW in Denmark Strait. Using least diluted PSW sample (station MG17), minimum dilution of Fram Strait PSW (fraction) = length C/D.

(Mauritzen et al., 2011). We are able to make such an estimate based on the Fram Strait endmembers and the tracer signature of RetAW samples collected at or just north of Denmark Strait. Endmembers for RAW and Fram Strait AAW (see orange and pink triangles in Figure 1 for geographical location) derived from previous measurement in Fram Strait (Wefing et al., 2019) are depicted on Figure 7. All samples measured north of Iceland for this study with the characteristics of RetAW are depicted as red diamonds. Ignoring samples that showed clear indications of substantial interleaving of PSW (half red diamond/half light blue circle markers), these form a relatively tight cluster in tracer space, particularly those measured in the core of the Atlantic layer of the EGC within Denmark Strait (mean value indicated by red triangle). If this RetAW formed from the pure mixing of Fram Strait AAW with RAW it would be expected to lie on a straight line (considering all uncertainties) between these two endmembers (solid line), however, it actually falls to the left. This is likely due to some mixing of RetAW with IW that circulates north and westward in Denmark Strait (Rudels et al., 1999). All measured samples with the characteristics of IW are shown as purple circles and an endmember for IW in Denmark Strait is indicated by a labeled purple triangle. We can remove the influence of this IW by projecting the Denmark Strait RetAW away from the IW endmember onto the line between Fram Strait AAW and RAW. We can thereby make an estimate of the contribution of RAW to RetAW from the lengths of lines A and B: the proportion of RAW to total RetAW is the ratio A/(A + B) = 41%. This value supports the estimate of RAW contribution of 28%–63% by Hattermann et al. (2016) over the 8%–37% by de Steur et al. (2014). The new estimate improves on methods attempting to measure the mixing of RAW with AAW in situ as it is based on the end-product of mixing and hence avoids some of the problems associated with dynamic environments as at Fram Strait. Even making a more conservative estimate based on the extremes of the 1-σ spreads on the Fram Strait AAW and RAW endmembers, RAW could be contributing 12%–64% to RetAW.

A final consideration of RetAW is that samples matching the hydrographic characteristics of this water mass are found not just close to the EGC but across the north and northeast of Iceland (stations SI8, LN3, LN6) and as far east as the Faroe-Shetland Channel (station MG30). The further away from the major conduit of RetAW to Iceland of the EGC, the less reliable the hydrographic characterization becomes at identifying Atlantic-origin water that has circulated around the Arctic Ocean or via Fram Strait. However, the tracer signature of these samples, especially at station MG30 (labeled on Figure 7), clearly identifies them as having the same tracer history as RetAW in the EGC with some modification by mixing with IW. This indicates a direct route of circulation from the EGC to the Faroe-Shetland Channel via the EIC (Blindheim & Rey, 2004; de Jong et al., 2018; Mauritzen, 1996) or NIIC (Casanova-Masjoan et al., 2020; Harden et al., 2016), and subsequently the IFSJ (Semper et al., 2020) which, as suggested before, justifies the classification of water at this location as Modified East Icelandic Water (Hátún et al., 2021; Read & Pollard, 1992). This unbroken conduit is important in that, with a potential density anomaly at this depth of $\sigma_\theta = 28.00$ kg/m^3, RetAW is dense enough ($\sigma_\theta > 27.8$ kg/m^3) (R. R. Dickson & Brown, 1994) to overflow at FBC and contribute to ISOW and hence the lower limb of AMOC via this route.

4.3. Integrity of the Surface East Greenland Current

The final endmember defined at Fram Strait is "Fram Strait PSW" (light blue triangle in Figure 1) and represents the tracer signature of PSW in the surface layer of the EGC in the strait. In Figure 7, samples with the hydrographic properties of PSW (light blue circles) in and just north of Denmark Strait lie in a noticeable line extending toward the lower left (line labeled "D"). The EGC carries PSW over RetAW and these have been shown to gradually mix during transit from Fram Strait to Denmark Strait (Jeansson et al., 2008; Mastropole et al., 2017). Additionally, Θ-S profiles of stations in and just north of Denmark Strait (Figure 3a) indicate the presence of IW recirculating westward from the NIIC in the strait. Therefore, this line in the dual tracer plot indicates mixing of PSW in the surface-EGC with RetAW and IW in variable amounts. In Figure 7, the distance of PSW samples between the Fram Strait PSW and the mixing line between the RetAW and IW endmembers indicates the amount of dilution of the original Fram Strait PSW. This is not necessarily proportional to the transit distance from Fram Strait but also represents whether the core or edge of the main surface EGC flow was sampled. Using the proportion of the length to the least diluted sample at station MG17 (line C) to the length of the RetAW-IW mixing line (line D), we can calculate that the PSW in the surface EGC retains up to 66% of its Fram Strait composition in or near the core surface-EGC.

The surface-EGC was not sampled south of Denmark Strait and hence we are unable to state if this coherence (i.e., the extent to which it remains undiluted) continues to the southern tip of Greenland. This integrity of the surface EGC is important from a tracer perspective as it carries the strongest tracer signature in the vicinity of Iceland, particularly of ^{129}I. The PSW carried by the surface EGC is estimated to contribute to about 6% of the volume of DSOW (Tanhua, Olsson, & Jeansson, 2005) and is seen to take part in deep convection in the Irminger Sea to contribute to LSW (Pickart et al., 2005; Våge, Pickart, Sarafanov, et al., 2011; Yashayaev et al., 2007) so even small contributions to these deep waters may be reflected in their measured tracer signatures (PSW contribution to DSOW is discussed in Section 4.6.1). The high influence of PSW on tracer signatures of samples affected by mixing with PSW can be seen where PSW was found interleaving with underlying water masses. This is evident in Θ-S profiles north of Iceland (Figures 3a and 3b) where shallowly-convected PSW is evident as cold, fresh excursions within RetAW or IW. These samples, plotting to the right of the RetAW-IW mixing line, are indicated on Figure 7 by markers of two corresponding shapes/colors (i.e., red diamonds/light blue circles).

4.4. The Provenance of Arctic Origin Water and Its Role in Overflow Formation

As previously discussed, the contribution of ArcW to the GSR overflows is difficult to estimate with hydrographic methods alone but transient tracers like ^{129}I–^{236}U can provide useful new insights. Samples with the hydrographic characteristics of ArcW have generally lower tracer concentrations than the previously discussed Atlantic-origin waters circulating in the Nordic Seas, therefore Figure 8 is a zoom-in of Figure 7 depicting ArcW

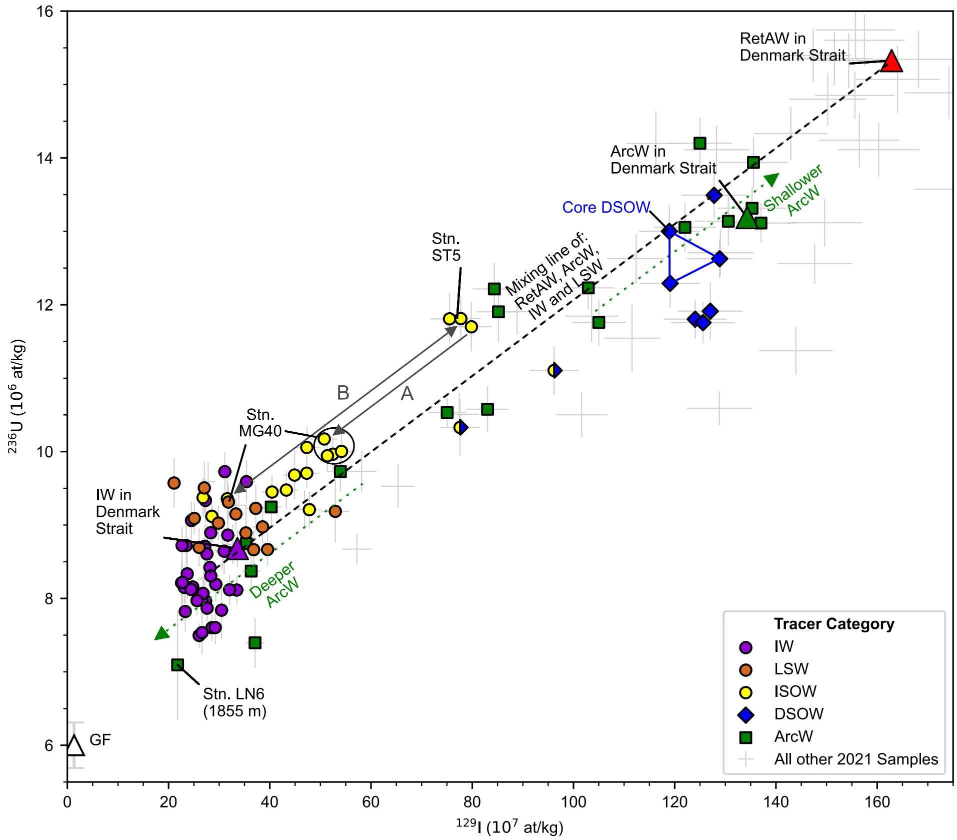

Figure 8. ^{129}I–^{236}U mixing plot (zoom of Figure 7) showing water masses and their mixing in the vicinity of Iceland and south of the GSR. Triangles represent endmembers defined from data in this study ("GF" is a current global fallout endmember as per Figures 4 and 7). All marker colors correspond with colors of water masses in Figures 1 and 2. Half-and-half ISOW-DSOW markers are samples that fall close to the Θ = 2°C demarcation criterion for these two masses where they flow together in the Irminger Sea as per Tanhua, Olsson, and Jeansson (2005) and tracers clearly indicate a mixture of both masses. Solid lines represent mixing of ISOW with LSW during transit from station ST5 to station MG40 using the tracer signature of LSW at station MG40. Entrainment of LSW by ISOW (fraction) between stations ST5 to MG40 = length A/B. The dotted lines signify the pattern of decreasing tracer values in Arctic water samples as depth increases, reaching its lowest point at the deepest measured sample (station LB6, 1,855 m, labeled).

and other water masses of lower tracer signatures. Endmembers for RetAW (red triangle) and ArcW (green triangle) in Denmark Strait have been defined based on samples measured in this study (RetAW: stations LB8 and LB10, 400–500 m; ArcW: station MG14, 400–600 m).

Three features of the ArcW samples (green squares) in Figure 8 provide important information on the ArcW layer, which can be used to aid in such an assessment: (a) they form an approximate straight line, (b) that line stretches between the RetAW endmember toward the global fallout endmember, and (c) they form a trend of decreasing tracer values with increasing depth (green dotted arrows). These indicate that ArcW is a product of the mixing of RetAW with another water mass with a global fallout signature, with the proportion of RetAW diminishing with depth. Both ends of this mixing line provide important information as to the source of the ArcW in the Iceland Sea. Several studies have estimated the source region of the dense waters feeding overflow of the GSR (e.g., Brakstad et al., 2023; Huang et al., 2020) but wherever the source locations (e.g., Greenland Sea, Iceland Sea, etc.), the mixing line in Figure 8 indicates that the water that is convected or mixed to form the ArcW measured in this study is predominantly RetAW. The lower end of the mixing line provides information on the source of the water into which the RetAW is mixing. It has a global fallout signature and so must have been at surface since the ^{236}U bomb spike of the 1950–60s. There is no indication, at least in this upper part of the ArcW layer, of any mixing with water with a natural background tracer signature (^{129}I = 1–2 x 10^7 at/kg, ^{236}U ≈ 0 at/kg) (Snyder et al., 2010; Steier et al., 2008) which would manifest on Figure 8 as ArcW samples with ^{236}U concentrations lower than the global fallout endmember. Hence we can state that all ArcW samples measured in this study are no older than ~60–70 years. Jeansson et al. (2023) found the mean age of ISDW (>1,500 m depth) to vary between 70 and >125 years between the 1980 and 2000s and have postulated that the periods of older apparent mean age are due to influxes of Arctic Ocean deep waters older than 175 years in ventilation age. There is no sign of such a component from the mixing line of ArcW samples in Figure 8 and the ArcW at <2,000 m must have an age <60–70 years. We acknowledge, however, that this assertion is based only on measurements of samples taken at the southern extreme of the Nordic Seas to a maximum depth of 1,855 m. Further sampling in the central Iceland and Greenland Seas may help to reveal different upper and lower component water masses of ArcW, including details of the deep and bottom water layers of ArcW that have been only partially sampled in this study.

Regardless of these considerations of the origin of the ArcW found just north of Iceland and the GSR, the tracercline in the ArcW layer has important implications when considering the role of ArcW in the formation of overflows. ArcW does not have a single endmember tracer signature but delivers a different signature depending on the depth of ArcW that acts as a source to downstream masses and this is considered below when discussing DSOW and ISOW.

4.5. Irminger Water

Three features of samples of IW on Figure 8 (purple circles) are notable: (a) they form a relatively tight cluster in the tracer space despite deriving from across the Irminger Sea and Iceland Basin, (b) their tracer content is considerably elevated above global fallout concentrations (about 10 times global fallout ^{129}I concentration) despite no obvious direct connectivity with the NRP source region, and (c) they have a tracer signature similar to the deepest ArcW samples measured in this study. How might these features be explained? As described earlier, Rudels et al. (1999) showed that some lower density RetAW passes over the East Greenland continental shelf instead of transiting the deepest section of the ridge at Denmark Strait and is subsequently observed to pass down the Greenland slope south of the strait to join DSOW (Pickart et al., 2005). If even a portion of this or the main overflow in the deepest strait (discussed below) is entrained into the IW of the Irminger Current that it passes through, IW will receive a continuous input of NRP tracer-loaded RetAW that will subsequently raise the tracer content of IW around the entire Sub-polar Gyre. This also explains why the tracer signature of IW is similar to that of ArcW at 1,500–2,000 m depth: it is produced by the mixing of a similar small portion of RetAW with water with a global fallout tracer content. This hypothesis of the "contamination" of the Sub-polar Gyre by contact with RetAW in the vicinity of Denmark Strait could be tested by further sampling at more distal locations around the Sub-polar Gyre.

4.6. Formation and Fate of DSOW and ISOW

4.6.1. Denmark Strait Overflow Water

To evaluate the water mass composition of DSOW, three stations have been selected along the southeast Greenland shelf break (Figure 2, MG6, MG8 and MG10), which intercept water with Θ-S properties characteristic of DSOW (Figure 3c). The concentration of both tracers is distinctly elevated in DSOW, particularly relative to the overlying upper column of IW in the Irminger Sea. On Figure 8, these form a relatively tight cluster (dark blue diamonds) with approximately the same signature as the upper ArcW layer north of the ridge. It should be noted that the most upstream station sampling DSOW has a bottom depth of 1,229 m and records overlying LSW and IW. This indicates that DSOW has already penetrated below IW and LSW at this location and likely entrained volumes of these water masses, with concomitant dilution of the DSOW tracer signature. The relatively tight cluster of tracer values recorded over ~800 km of DSOW transit supports the position that after significant entrainment of IW immediately after overflow, the characteristics of DSOW remain relatively stable thereafter (R. R. Dickson & Brown, 1994; B. Dickson et al., 2008).

Samples representing four of the possible contributors to DSOW, namely RetAW, ArcW, IW and LSW, fall approximately along a (black dashed) line on Figure 8. Three samples that were most unequivocally in the core of DSOW according to Θ-S profiles are marked with a blue triangle that also intercepts the mixing line of these four inputs to DSOW. Samples of DSOW that fall below the line must have an input of PSW (already diluted with RetAW or IW and therefore falling on mixing line D in Figure 7) and their distance to the Fram Strait PSW endmember on Figure 7 indicates about 5% contribution of undiluted Fram Strait PSW. Calculating the proportion of the four remaining inputs to DSOW is complicated by their orientation on a single line and this represents one of the potential deficiencies of this dual tracer method when estimating mixing of certain water masses. A previous estimate of the composition of DSOW at this downstream location suggests DSOW is composed of approximately one third each of RetAW and ArcW, 6% PSW, the remainder coming from a combination of IW and LSW (Tanhua, Olsson, & Jeansson, 2005). As previously described, the tracer signature of the contribution of ArcW to DSOW depends on the density level in the Arctic-origin layer that is actually contributing to the overflow. It should be noted that the lowest density layer of ArcW only just reaches the Denmark Strait sill at 660 m depth; in fact, no ArcW was detected during measurement in winter 2021 (Figure 3a, stations LB8 and LB10). However, aspiration of the top layer of ArcW from below the level of the sill has been previously recorded (Harden et al., 2016) so we can assume this upper layer is able to contribute to overflow even if not measured at the sill on any one day. The tracer signature of ArcW actually measured at the sill in summer 2021 (Figure 3a, station MG14) is indicated on Figure 8 by the green endmember triangle and we can therefore assume this position along the mixing line is the signature of any contribution of ArcW to DSOW. If we treat IW and LSW as having the same tracer signature (at the lower end of the mixing line) and group their contribution together, we still have three unknown contributing portions, one too many to solve the flow mass balance using the positions of the masses along the mixing line. We can run two scenarios assuming each of RetAW and ArcW constitute one third of DSOW (as per Tanhua, Olsson, and Jeansson (2005)). A mass balance based on the positions of these three inputs on the mixing line produces possible proportions of RetAW = 33–43%, ArcW = 33–45% and (LSW + IW) = 21–24%. This is certainly commensurate with the overall evaluation by Tanhua, Olsson, and Jeansson (2005), especially given the 15%–20% temporal variability in their estimate.

4.6.2. Iceland-Scotland Overflow Water

An attempt to estimate the water mass contributions to ISOW can be made using their location on Figure 8 (yellow circles). Samples identified as ISOW, with the exception of those from station ST5 (labeled), have tracer signatures plotting mostly in another tight cluster but with concentrations lower than those of DSOW, particularly of ^{129}I, which is less than half that of DSOW. These values are remarkable consistent for samples sourced from as far east as station MG38 in the Iceland Basin to station MG6 in the Irminger Basin and indicative of the highly advective nature of the transit of ISOW from the Iceland to Irminger Basins around and through the Reykjanes Ridge. A noticeable exception are the three samples from station ST5 with distinctly higher ^{129}I and ^{236}U, only 230 km upstream from station MG38 (labeled with station name in Figure 8). Whilst this may reflect some "leakage" of dense ArcW water across the western Iceland-Faroe ridge (Hansen & Østerhus, 2000), another explanation can be found by observing where LSW has been detected south of Iceland. Station ST5 has a bottom depth of 1,160 m where water with the Θ-S characteristics of ISOW in the Iceland Basin (García-Ibáñez et al., 2018) is identified but no salinity minimum to indicate any overlying LSW (Figure 3d). By the next station downstream (MG38), the bottom depth has increased to 1,575 m and there is a clear salinity minimum and oxygen maximum indicating LSW overlying denser ISOW. This means that during this rapid increase in depth from station ST5 to MG38, ISOW has commenced passing beneath the LSW layer south of Iceland. We can therefore interpret the dramatic change in tracer signature of ISOW samples on Figure 8 as entrainment of LSW by ISOW during penetration of this layer. By considering the tracer signatures of LSW and ISOW after ISOW has completed passing through and below the LSW layer (station MG40), we can evaluate how much LSW is entrained by ISOW during this transit. From the ratio of lengths A/B on the plot, the tracers indicate that ISOW entrains approximately 60% LSW in the process. This compares with a previous estimate based on nutrient and CFC tracers that ISOW entrains 46% LSW at this point in its course through the Atlantic (Fogelqvist et al., 2003). Unfortunately, the same study shows that ISOW is already considerably modified by entrainment of North East Atlantic Water between overflow at Faroe Bank Channel and the location of station ST5 so we are unable to use the tracers to estimate the water masses that go into the formation of the original overflow mass (Faroe Bank Channel Overflow). However, we can conclude that the lower tracer signature of ISOW compared with that of DSOW, even before any dilution with LSW, indicates that ISOW receives a contribution from deeper in the tracercline of the ArcW layer than DSOW, as is expected from the deeper point of overflow in FBC (840 m) compared with at Denmark Strait (660 m). This is commensurate with previous estimates of a substantial contribution to ISOW of NSDW, a deep component of ArcW (Turrell et al., 1999).

4.6.3. Disentangling ISOW and DSOW

The very different tracer signatures of DSOW and ISOW become particularly useful where these two masses come together south of Denmark Strait and flow together, ISOW above DSOW, as the incipient DWBC. From

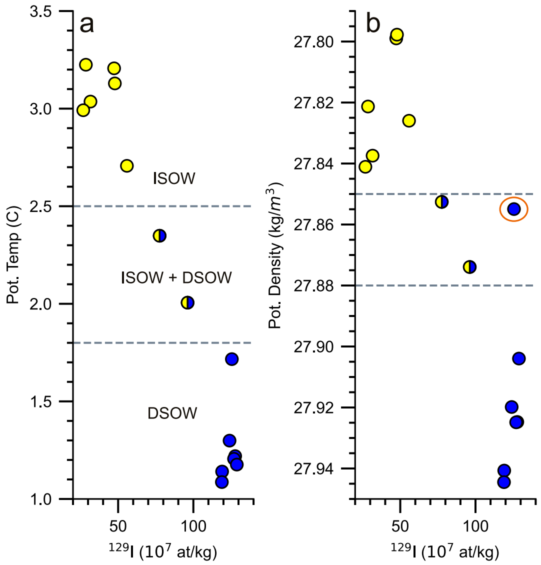

Figure 9. Plots of ^{129}I against potential temperature (a) and potential density anomaly (b) for all samples characterized as ISOW, DSOW (or mixture of both) in the Irminger Sea. As per previous figures, colors are: yellow: ISOW, dark blue: DSOW, with half-and-half indicating where tracers show them to be a mix. Dashed lines in (a) are recommended temperature range to differentiate between ISOW, DSOW and their mixed zone where they flow in contact in the DWBC. Dashed lines in (b) are previously proposed potential densities for demarking ISOW from DSOW. The criterion $\sigma_{\theta(\mathrm{ISOW})} \leq 27.88$ kg/m^3 incorrectly identifies a sample as ISOW that tracers clearly show is DSOW (orange circle) and so the $\sigma_{\theta(\mathrm{ISOW})} \leq 27.85$ kg/m^3 criterion is recommended.

this region in the Irminger Sea, the two overflow plumes become difficult to distinguish using hydrographic criteria. Several demarcation criteria have been proposed, such as density anomalies (σ_θ) between 27.85 and 27.88 kg/m^3 (B. Dickson et al., 2008; R. R. Dickson & Brown, 1994; Stramma et al., 2004; Tanhua, Bulsiewicz, & Rhein, 2005) and/or potential temperatures between 1.5 and 2.5°C (Tanhua, Bulsiewicz, & Rhein, 2005; Tanhua, Olsson, & Jeansson, 2005). When initially categorizing samples from the Irminger Sea in this study, we used the criteria that $\Theta_{(\mathrm{DSOW})} \leq 2°\mathrm{C} < \Theta_{(\mathrm{ISOW})}$. Once plotted on Figure 8, it becomes clear that the ^{129}I–^{236}U dual tracer is much better than the physical properties at differentiating ISOW from DSOW samples, even when ISOW is circulating immediately above and in contact with DSOW. It is also possible to see where the two layers are intermixing and two samples that fall between the clusters of ISOW and DSOW (Figure 8, half yellow circle/blue diamond markers), which had potential temperatures of 2.0°C and 2.4°C, are clearly in this intermixing layer.

To compare the utility of using even ^{129}I alone to distinguish ISOW from DSOW in this critical region of the incipient DWBC, Figure 9 shows the ^{129}I concentrations for all samples in the Irminger Sea plotted against potential temperature (a) and potential density (b). From Figure 9a, it is clear that, whilst using a potential temperature demarcation of 2°C is suitable as a "rule of thumb" to differentiate between ISOW and DSOW, a better criterion is to assume that a potential temperature range of 1.8–2.5°C will characterize the mixing zone of the two overflows. Using a potential density demarcation (Figure 9b) of $\sigma_\theta = 27.88$ kg/m^3 appears to wrongly characterize at least one sample in this study as ISOW that has tracer values clearly identifying it as DSOW (circled in orange). A criterion of $\sigma_{\theta(\mathrm{ISOW})} \leq 27.85$ kg/m^3 correctly demarcates the overflows but cannot identify where the overflows may be mixing at σ_θ of 27.85–27.88 kg/m^3. We therefore propose that these tracers, especially ^{129}I, are the best method for tracing the fate of these overflow plumes as and after they come together in the Irminger Sea. The tracer signature of LSW (Figure 8, brown circles), whilst somewhat overlapping with that of ISOW, may be distinct enough to allow separate tracing of all three major components of the DWBC downstream into the Labrador Sea and beyond into the wider North Atlantic basin with better fidelity than using hydrographic properties alone.

5. Conclusions

The artificial radionuclide ^{129}I–^{236}U dual tracer demonstrates robust potential as a tracer of ocean circulation from the Arctic Ocean to the Subpolar North Atlantic in the vicinity of the Iceland gateway due to its well-defined release profile and high resolution between different water masses. In particular, the surface and Atlantic waters passing through Fram Strait from different upstream sources exhibit highly unique ^{129}I–^{236}U tracer signatures. Such high variance in tracer concentrations allows estimation of mixing contributions for a number of key water masses in the region and tracing of their major circulatory pathways, albeit limited where several water masses have very similar tracer signatures or fall on the same mixing line in dual-tracer space.

The tracers indicate that at the time under investigation (2016) at least half of the Arctic Atlantic Water exiting the Arctic Ocean via the East Greenland Current (EGC) came from the Atlantic branch that circulated via the Canada Basin as opposed to via the shorter routes of the Makarov and Amundsen Basins. At Fram Strait, they also provide an independent tracer-based estimate of the contribution of Recirculating Atlantic Water to the Return Atlantic Water in the EGC of about 40% (12%–64%). The product Return Atlantic Water carried by the EGC has been traced to Denmark Strait but also to the north of Iceland via the East Iceland Current and as far east as the Faroe-Shetland Channel, where it can contribute to Iceland-Scotland Overflow Water (ISOW). Polar Surface Water, carried by the surface EGC, exhibits particularly high concentrations of ^{129}I and ^{236}U. This means the mixing of this surface water mass with Return Atlantic Water (RetAW) and Irminger Water (IW) on approach to Denmark Strait is easily traced and we see that the core surface-EGC is diluted with RetAW and IW by a maximum of 33% before reaching Denmark Strait. The tracers indicate that water of Arctic origin circulating in the southern Iceland

and Norwegian Seas is a mixture of return Atlantic Water convected or mixed with water with a global fallout tracer signature. This precludes any substantial contribution of old, dense waters from the Arctic Ocean to the Arctic-origin Water in the sample area and period of sampling, though sampling in the deeper Nordic Seas basins would serve to clarify this assessment.

Whilst the tracers and currently available data cannot directly estimate the proportions of major water masses that contribute to production of Denmark Strait Overflow Water (DSOW), the tracer signatures of the water masses involved are in agreement with a previous estimate of the constituents of DSOW. The tracers are able to make a confident estimate of the volume of Labrador Sea Water (LSW) entrained by ISOW as it penetrates this layer (60%), and show that ISOW remains remarkably coherent, traveling advectively around the Iceland and Irminger Basins to join the incipient Deep Western Boundary Current. ISOW and DSOW have such distinct tracer signatures that the ^{129}I concentration is a better way to differentiate these plumes than using temperature or density when they commence flowing together southeast of Greenland. Given the distinctive tracer signature of LSW from the overflows, it should be possible to trace all three components of the Deep Western Boundary Current (LSW, and DSOW) downstream into the Labrador Sea and main North Atlantic basin with appropriate sampling in those regions.

Data Availability Statement

Radioisotope and hydrographic data are available at MARIS (Marine Radioactivity Information System): https://maris.iaea.org/datasets.

Acknowledgments
The TITANICA project (PI Núria Casacuberta) has received funding from the European Research Council (ERC) under the European Union's Horizon 2020 research and innovation programme (ERC-2020-COG 101001451) and from the Swiss National Science Foundation (PR00P2-193091-TRACEATLANTIC). The authors thank two anonymous reviewers for their insightful comments, which improved the manuscript. We also thank the captain, officers and crew of the RV Pelagia expedition 64PE74 (MetalGate), especially Patrick Laan, Rebecca Zitoun and Cuun Koek for their assistance with sampling; and the captain and crew of the RV Bjarni Sæmundsson during the MFRI cruise of February 2021, particularly Alice Benoit-Cattin, Jacek Sliwinski and Magnús Danielsen. Thanks to Kayley Kündig for laboratory support, and all the staff and technicians of the Laboratory of Ion-beam Physics who contributed to this project. Selection and interpretation of radioisotope data from Fram Strait and the Arctic Ocean was achieved with the generous help of Anne-Marie Wefing and Elena Chamizo Calvo. Open access funding provided by Eidgenossische Technische Hochschule Zurich.

References

Aldahan, A., Alfimov, V., & Possnert, G. (2007). ^{129}I anthropogenic budget: Major sources and sinks. *Applied Geochemistry*, *22*(3), 606–618. https://doi.org/10.1016/j.apgeochem.2006.12.006

Blindheim, J., & Rey, F. (2004). Water-mass formation and distribution in the Nordic Seas during the 1990s. *ICES Journal of Marine Science*, *61*(5), 846–863. https://doi.org/10.1016/j.icesjms.2004.05.003

Brakstad, A., Gebbie, G., Våge, K., Jeansson, E., & Ólafsdóttir, S. R. (2023). Formation and pathways of dense water in the Nordic Seas based on a regional inversion. *Progress in Oceanography*, *212*, 102981. https://doi.org/10.1016/j.pocean.2023.102981

Brambilla, E., Talley, L. D., & Robbins, P. E. (2008). Subpolar mode water in the northeastern Atlantic: 2. Origin and transformation. *Journal of Geophysical Research*, *113*(C4), 2006JC004063. https://doi.org/10.1029/2006JC004063

Casacuberta, N., Christl, M., Lachner, J., van der Loeff, M. R., Masqué, P., & Synal, H.-A. (2014). A first transect of ^{236}U in the North Atlantic Ocean. *Geochimica et Cosmochimica Acta*, *133*, 34–46. https://doi.org/10.1016/j.gca.2014.02.012

Casacuberta, N., Christl, M., Vockenhuber, C., Wefing, A.-M., Wacker, L., Masqué, P., et al. (2018). Tracing the three Atlantic branches entering the Arctic Ocean with ^{129}I and ^{236}U. *Journal of Geophysical Research: Oceans*, *123*(9), 6909–6921. https://doi.org/10.1029/2018JC014168

Casacuberta, N., Masqué, P., Henderson, G., Rutgers van-der-Loeff, M., Bauch, D., Vockenhuber, C., et al. (2016). First ^{236}U data from the Arctic Ocean and use of ^{236}U/^{238}U and ^{129}I/^{236}U as a new dual tracer. *Earth and Planetary Science Letters*, *440*, 127–134. https://doi.org/10.1016/j.epsl.2016.02.020

Casacuberta, N., & Smith, J. N. (2023). Nuclear reprocessing tracers illuminate flow features and connectivity between the Arctic and subpolar North Atlantic oceans. *Annual Review of Marine Science*, *15*(1), 203–221. https://doi.org/10.1146/annurev-marine-032122-112413

Casanova-Masjoan, M., Pérez-Hernández, M. D., Pickart, R. S., Valdimarsson, H., Ólafsdóttir, S. R., Macrander, A., et al. (2020). Along-stream, seasonal, and interannual variability of the north Icelandic irminger current and east Icelandic current around Iceland. *Journal of Geophysical Research: Oceans*, *125*(9), e2020JC016283. https://doi.org/10.1029/2020JC016283

Chamizo, E., Christl, M., López-Lora, M., Casacuberta, N., Wefing, A.-M., & Kenna, T. C. (2022). The Potential of ^{233}U/^{236}U as a water mass tracer in the Arctic Ocean. *Journal of Geophysical Research: Oceans*, *127*(3), e2021JC017790. https://doi.org/10.1029/2021JC017790

Christl, M., Casacuberta, N., Lachner, J., Herrmann, J., & Synal, H.-A. (2017). Anthropogenic ^{236} U in the North Sea – A closer look into a source region. *Environmental Science & Technology*, *51*(21), 12146–12153. https://doi.org/10.1021/acs.est.7b03168

Christl, M., Casacuberta, N., Vockenhuber, C., Elsässer, C., Bailly du Bois, P., Herrmann, J., & Synal, H. (2015). Reconstruction of the ^{236}U input function for the Northeast Atlantic Ocean: Implications for ^{129}I/^{236}U and ^{236}U/^{238}U -based tracer ages. *Journal of Geophysical Research: Oceans*, *120*(11), 7282–7299. https://doi.org/10.1002/2015JC011116

Christl, M., Gautschi, P., Maxeiner, S., Müller, A. M., Vockenhuber, C., & Synal, H.-A. (2023). ^{236}U analyses with the ETH Zurich MILEA prototype system. *Nuclear Instruments and Methods in Physics Research Section B: Beam Interactions with Materials and Atoms*, *534*, 61–71. https://doi.org/10.1016/j.nimb.2022.11.009

Christl, M., Vockenhuber, C., Kubik, P. W., Wacker, L., Lachner, J., Alfimov, V., & Synal, H.-A. (2013). The ETH Zurich AMS facilities: Performance parameters and reference materials. *Nuclear Instruments and Methods in Physics Research Section B: Beam Interactions with Materials and Atoms*, *294*, 29–38. https://doi.org/10.1016/j.nimb.2012.03.004

Clarke, R. A., & Gascard, J.-C. (1983). The formation of labrador sea water. Part I: Large-scale processes. *Journal of Physical Oceanography*, *13*(10), 1764–1778. https://doi.org/10.1175/1520-0485(1983)013<1764:TFOLSW>2.0.CO;2

de Jong, M. F., Søiland, H., Bower, A. S., & Furey, H. H. (2018). The subsurface circulation of the Iceland Sea observed with RAFOS floats. *Deep Sea Research Part I: Oceanographic Research Papers*, *141*, 1–10. https://doi.org/10.1016/j.dsr.2018.07.008

de Steur, L., Hansen, E., Mauritzen, C., Beszczynska-Möller, A., & Fahrbach, E. (2014). Impact of recirculation on the East Greenland Current in Fram Strait: Results from moored current meter measurements between 1997 and 2009. *Deep Sea Research Part I: Oceanographic Research Papers*, *92*, 26–40. https://doi.org/10.1016/j.dsr.2014.05.018

Dickson, B., Dye, S., Jónsson, S., Köhl, A., Macrander, A., Marnela, M., et al. (2008). The overflow flux west of Iceland: Variability, origins and forcing. In R. R. Dickson, J. Meincke, & P. Rhines (Eds.), *Arctic–subarctic ocean fluxes* (pp. 443–474). Springer. https://doi.org/10.1007/978-1-4020-6774-7_20

Dickson, R. R., & Brown, J. (1994). The production of North Atlantic Deep Water: Sources, rates, and pathways. *Journal of Geophysical Research*, *99*(C6), 12319–12341. https://doi.org/10.1029/94JC00530

Edmonds, H. N., Zhou, Z. Q., Raisbeck, G. M., Yiou, F., Kilius, L., & Edmond, J. M. (2001). Distribution and behavior of anthropogenic ^{129}I in water masses ventilating the North Atlantic Ocean. *Journal of Geophysical Research*, *106*(C4), 6881–6894. https://doi.org/10.1029/1999JC000282

Fogelqvist, E., Blindheim, J., Tanhua, T., Østerhus, S., Buch, E., & Rey, F. (2003). Greenland–Scotland overflow studied by hydro-chemical multivariate analysis. *Deep Sea Research Part I: Oceanographic Research Papers*, *50*(1), 73–102. https://doi.org/10.1016/S0967-0637(02)00131-0

Frajka-Williams, E., Ansorge, I. J., Baehr, J., Bryden, H. L., Chidichimo, M. P., Cunningham, S. A., et al. (2019). Atlantic Meridional Overturning Circulation: Observed transport and variability. *Frontiers in Marine Science*, *6*, 260. https://doi.org/10.3389/fmars.2019.00260

García-Ibáñez, M. I., Pérez, F. F., Lherminier, P., Zunino, P., Mercier, H., & Tréguer, P. (2018). Water mass distributions and transports for the 2014 GEOVIDE cruise in the North Atlantic. *Biogeosciences*, *15*(7), 2075–2090. https://doi.org/10.5194/bg-15-2075-2018

Hansen, B., & Østerhus, S. (2000). North Atlantic–Nordic Seas exchanges. *Progress in Oceanography*, *45*(2), 109–208. https://doi.org/10.1016/S0079-6611(99)00052-X

Harden, B. E., Pickart, R. S., Valdimarsson, H., Våge, K., de Steur, L., Richards, C., et al. (2016). Upstream sources of the Denmark Strait Overflow: Observations from a high-resolution mooring array. *Deep Sea Research Part I: Oceanographic Research Papers*, *112*, 94–112. https://doi.org/10.1016/j.dsr.2016.02.007

Hattermann, T., Isachsen, P. E., von Appen, W., Albretsen, J., & Sundfjord, A. (2016). Eddy-driven recirculation of Atlantic Water in Fram Strait. *Geophysical Research Letters*, *43*(7), 3406–3414. https://doi.org/10.1002/2016GL068323

Hátún, H., Chafik, L., & Larsen, K. M. H. (2021). The Norwegian Sea Gyre – A Regulator of Iceland-Scotland Ridge Exchanges. *Frontiers in Marine Science*, *8*, 694614. https://doi.org/10.3389/fmars.2021.694614

Håvik, L., Pickart, R. S., Våge, K., Torres, D., Thurnherr, A. M., Beszczynska-Möller, A., et al. (2017). Evolution of the East Greenland Current from Fram Strait to Denmark S trait: Synoptic measurements from summer 2012. *Journal of Geophysical Research: Oceans*, *122*(3), 1974–1994. https://doi.org/10.1002/2016JC012228

He, P., Hou, X., Aldahan, A., Possnert, G., & Yi, P. (2013). Iodine isotopes species fingerprinting environmental conditions in surface water along the northeastern Atlantic Ocean. *Scientific Reports*, *3*(1), 2685. https://doi.org/10.1038/srep02685

Huang, J., Pickart, R. S., Huang, R. X., Lin, P., Brakstad, A., & Xu, F. (2020). Sources and upstream pathways of the densest overflow water in the Nordic Seas. *Nature Communications*, *11*(1), 5389. https://doi.org/10.1038/s41467-020-19050-y

Huang, J., Pickart, R. S., Valdimarsson, H., Lin, P., Spall, M. A., & Xu, F. (2019). Structure and variability of the North Icelandic jet from two years of mooring data. *Journal of Geophysical Research: Oceans*, *124*(6), 3987–4002. https://doi.org/10.1029/2019JC015134

Jeansson, E., Jutterström, S., Rudels, B., Anderson, L. G., Anders Olsson, K., Jones, E. P., et al. (2008). Sources to the East Greenland Current and its contribution to the Denmark Strait Overflow. *Progress in Oceanography*, *78*(1), 12–28. https://doi.org/10.1016/j.pocean.2007.08.031

Jeansson, E., Tanhua, T., Olsen, A., Smethie, W. M., Rajasakaren, B., Ólafsdóttir, S. R., & Ólafsson, J. (2023). Decadal changes in ventilation and anthropogenic carbon in the Nordic Seas. *Journal of Geophysical Research: Oceans*, *128*(3), e2022JC019318. https://doi.org/10.1029/2022JC019318

Jochumsen, K., Moritz, M., Nunes, N., Quadfasel, D., Larsen, K. M. H., Hansen, B., et al. (2017). Revised transport estimates of the Denmark Strait overflow. *Journal of Geophysical Research: Oceans*, *122*(4), 3434–3450. https://doi.org/10.1002/2017JC012803

Jochumsen, K., Quadfasel, D., Valdimarsson, H., & Jónsson, S. (2012). Variability of the Denmark Strait overflow: Moored time series from 1996–2011. *Journal of Geophysical Research*, *117*(C12), 2012JC008244. https://doi.org/10.1029/2012JC008244

Johnson, G. C. (2008). Quantifying Antarctic bottom water and North Atlantic deep water volumes. *Journal of Geophysical Research*, *113*(C5), 2007JC004477. https://doi.org/10.1029/2007JC004477

Jónsson, S., & Valdimarsson, H. (2004). A new path for the Denmark Strait overflow water from the Iceland Sea to Denmark Strait. *Geophysical Research Letters*, *31*(3), 2003GL019214. https://doi.org/10.1029/2003GL019214

Lin, P., Pickart, R. S., Jochumsen, K., Moore, G. W. K., Valdimarsson, H., Fristedt, T., & Pratt, L. J. (2020). Kinematic structure and dynamics of the Denmark strait overflow from ship-based observations. *Journal of Physical Oceanography*, *50*(11), 3235–3251. https://doi.org/10.1175/JPO-D-20-0095.1

Liu, M., & Tanhua, T. (2021). Water masses in the Atlantic Ocean: Characteristics and distributions. *Ocean Science*, *17*(2), 463–486. https://doi.org/10.5194/os-17-463-2021

Lozier, M. S. (2023). Overturning in the Subpolar North Atlantic: A review. *Philosophical Transactions of the Royal Society A: Mathematical, Physical & Engineering Sciences*, *381*(2262), 20220191. https://doi.org/10.1098/rsta.2022.0191

Macrander, A., Send, U., Valdimarsson, H., Jónsson, S., & Käse, R. H. (2005). Interannual changes in the overflow from the Nordic Seas into the Atlantic Ocean through Denmark Strait. *Geophysical Research Letters*, *32*(6), 2004GL021463. https://doi.org/10.1029/2004GL021463

Macrander, A., Valdimarsson, H., & Jónsson, S. (2014). Improved transport estimate of the East Icelandic Current 2002–2012. *Journal of Geophysical Research: Oceans*, *119*(6), 3407–3424. https://doi.org/10.1002/2013JC009517

Mastropole, D., Pickart, R. S., Valdimarsson, H., Våge, K., Jochumsen, K., & Girton, J. (2017). On the hydrography of Denmark Strait. *Journal of Geophysical Research: Oceans*, *122*(1), 306–321. https://doi.org/10.1002/2016JC012007

Mauritzen, C. (1996). Production of dense overflow waters feeding the North Atlantic across the Greenland-Scotland Ridge. Part 1: Evidence for a revised circulation scheme. *Deep Sea Research Part I: Oceanographic Research Papers*, *43*(6), 769–806. https://doi.org/10.1016/0967-0637(96)00037-4

Mauritzen, C., Hansen, E., Andersson, M., Berx, B., Beszczynska-Möller, A., Burud, I., et al. (2011). Closing the loop – Approaches to monitoring the state of the Arctic Mediterranean during the International Polar Year 2007–2008. *Progress in Oceanography*, *90*(1–4), 62–89. https://doi.org/10.1016/j.pocean.2011.02.010

Pickart, R. S., Torres, D. J., & Fratantoni, P. S. (2005). The East Greenland spill jet. *Journal of Physical Oceanography*, *35*(6), 1037–1053. https://doi.org/10.1175/jpo2734.1

Raisbeck, G. M., & Yiou, F. (1999). 129I in the oceans: Origins and applications. *Science of the Total Environment*, *237–238*, 31–41. https://doi.org/10.1016/S0048-9697(99)00122-9

Read, J. F., & Pollard, R. T. (1992). Water masses in the region of the Iceland–Færoes Front. *Journal of Physical Oceanography*, *22*(11), 1365–1378. https://doi.org/10.1175/1520-0485(1992)022<1365:WMITRO>2.0.CO;2

Rudels, B. (2002). The East Greenland Current and its contribution to the Denmark Strait Overflow. *ICES Journal of Marine Science*, *59*(6), 1133–1154. https://doi.org/10.1006/jmsc.2002.1284

Rudels, B. (2022). The circulation and transformations of Atlantic water in the Arctic Mediterranean Sea. In *The physical oceanography of the Arctic Mediterranean Sea* (pp. 211–276). Elsevier. https://doi.org/10.1016/B978-0-12-816930-8.00010-4

Rudels, B., Björk, G., Nilsson, J., Winsor, P., Lake, I., & Nohr, C. (2005). The interaction between waters from the Arctic Ocean and the Nordic Seas north of Fram Strait and along the East Greenland Current: Results from the Arctic Ocean-02 Oden expedition. *Journal of Marine Systems*, *55*(1–2), 1–30. https://doi.org/10.1016/j.jmarsys.2004.06.008

Rudels, B., Eriksson, P., Grönvall, H., Hietala, R., & Launiainen, J. (1999). Hydrographic observations in Denmark Strait in fall 1997, and their implications for the entrainment into the overflow plume. *Geophysical Research Letters*, *26*(9), 1325–1328. https://doi.org/10.1029/1999GL900212

Rudels, B., Korhonen, M., Schauer, U., Pisarev, S., Rabe, B., & Wisotzki, A. (2015). Circulation and transformation of Atlantic water in the Eurasian Basin and the contribution of the Fram Strait inflow branch to the Arctic Ocean heat budget. *Progress in Oceanography*, *132*, 128–152. https://doi.org/10.1016/j.pocean.2014.04.003

Sakaguchi, A., Kadokura, A., Steier, P., Takahashi, Y., Shizuma, K., Hoshi, M., et al. (2012). Uranium-236 as a new oceanic tracer: A first depth profile in the Japan Sea and comparison with caesium-137. *Earth and Planetary Science Letters*, *333*(334), 165–170. https://doi.org/10.1016/j.epsl.2012.04.004

Schaffer, J., von Appen, W., Dodd, P. A., Hofstede, C., Mayer, C., de Steur, L., & Kanzow, T. (2017). Warm water pathways toward Nioghalvfjerdsfjorden Glacier, Northeast Greenland. *Journal of Geophysical Research: Oceans*, *122*(5), 4004–4020. https://doi.org/10.1002/2016JC012462

Semper, S., Pickart, R. S., Våge, K., Larsen, K. M. H., Hátún, H., & Hansen, B. (2020). The Iceland-Faroe Slope Jet: A conduit for dense water toward the Faroe Bank Channel overflow. *Nature Communications*, *11*(1), 5390. https://doi.org/10.1038/s41467-020-19049-5

Semper, S., Våge, K., Pickart, R. S., Jónsson, S., & Valdimarsson, H. (2022). Evolution and transformation of the north Icelandic irminger current along the North Iceland Shelf. *Journal of Geophysical Research: Oceans*, *127*(3), e2021JC017700. https://doi.org/10.1029/2021JC017700

Semper, S., Våge, K., Pickart, R. S., Valdimarsson, H., Torres, D. J., & Jónsson, S. (2019). The emergence of the North Icelandic jet and its evolution from Northeast Iceland to Denmark Strait. *Journal of Physical Oceanography*, *49*(10), 2499–2521. https://doi.org/10.1175/JPO-D-19-0088.1

Smith, J. N., Jones, E. P., Moran, S. B., Smethie, W. M., & Kieser, W. E. (2005). Iodine 129/CFC 11 transit times for Denmark Strait Overflow Water in the Labrador and Irminger Seas. *Journal of Geophysical Research*, *110*(C5), 2004JC002516. https://doi.org/10.1029/2004JC002516

Smith, J. N., McLaughlin, F. A., Smethie, W. M., Moran, S. B., & Lepore, K. (2011). Iodine-129, ^{137}Cs, and CFC-11 tracer transit time distributions in the Arctic Ocean. *Journal of Geophysical Research*, *116*(C4), C04024. https://doi.org/10.1029/2010JC006471

Snyder, G., Aldahan, A., & Possnert, G. (2010). Global distribution and long-term fate of anthropogenic ^{129}I in marine and surface water reservoirs. *Geochemistry, Geophysics, Geosystems*, *11*(4), 2009GC002910. https://doi.org/10.1029/2009GC002910

Steier, P., Bichler, M., Keith Fifield, L., Golser, R., Kutschera, W., Priller, A., et al. (2008). Natural and anthropogenic ^{236}U in environmental samples. *Nuclear Instruments and Methods in Physics Research Section B: Beam Interactions with Materials and Atoms*, *266*(10), 2246–2250. https://doi.org/10.1016/j.nimb.2008.03.002

Stramma, L., Kieke, D., Rhein, M., Schott, F., Yashayaev, I., & Koltermann, K. P. (2004). Deep water changes at the western boundary of the subpolar North Atlantic during 1996 to 2001. *Deep Sea Research Part I: Oceanographic Research Papers*, *51*(8), 1033–1056. https://doi.org/10.1016/j.dsr.2004.04.001

Swift, J. H. (1984). The circulation of the Denmark Strait and Iceland-Scotland overflow waters in the North Atlantic. *Deep-Sea Research, Part A: Oceanographic Research Papers*, *31*(11), 1339–1355. https://doi.org/10.1016/0198-0149(84)90005-0

Swift, J. H., & Aagaard, K. (1981). Seasonal transitions and water mass formation in the Iceland and Greenland seas. *Deep-Sea Research, Part A: Oceanographic Research Papers*, *28*(10), 1107–1129. https://doi.org/10.1016/0198-0149(81)90050-9

Tanhua, T., Bulsiewicz, K., & Rhein, M. (2005). Spreading of overflow water from the Greenland to the Labrador Sea. *Geophysical Research Letters*, *32*(10), 2005GL022700. https://doi.org/10.1029/2005GL022700

Tanhua, T., Olsson, K. A., & Jeansson, E. (2005). Formation of Denmark Strait overflow water and its hydro-chemical composition. *Journal of Marine Systems*, *57*(3–4), 264–288. https://doi.org/10.1016/j.jmarsys.2005.05.003

Thierry, V., de Boisséson, E., & Mercier, H. (2008). Interannual variability of the subpolar mode water properties over the Reykjanes Ridge during 1990–2006. *Journal of Geophysical Research*, *113*(C4), 2007JC004443. https://doi.org/10.1029/2007JC004443

Turrell, W. R., Slesser, G., Adams, R. D., Payne, R., & Gillibrand, P. A. (1999). Decadal variability in the composition of Faroe Shetland Channel bottom water. *Deep Sea Research Part I: Oceanographic Research Papers*, *46*(1), 1–25. https://doi.org/10.1016/S0967-0637(98)00067-3

Våge, K., Moore, G. W. K., Jónsson, S., & Valdimarsson, H. (2015). Water mass transformation in the Iceland Sea. *Deep Sea Research Part I: Oceanographic Research Papers*, *101*, 98–109. https://doi.org/10.1016/j.dsr.2015.04.001

Våge, K., Pickart, R. S., Sarafanov, A., Knutsen, Ø., Mercier, H., Lherminier, P., et al. (2011). The Irminger Gyre: Circulation, convection, and interannual variability. *Deep Sea Research Part I: Oceanographic Research Papers*, *58*(5), 590–614. https://doi.org/10.1016/j.dsr.2011.03.001

Våge, K., Pickart, R. S., Spall, M. A., Moore, G. W. K., Valdimarsson, H., Torres, D. J., et al. (2013). Revised circulation scheme north of the Denmark Strait. *Deep Sea Research Part I: Oceanographic Research Papers*, *79*, 20–39. https://doi.org/10.1016/j.dsr.2013.05.007

Våge, K., Pickart, R. S., Spall, M. A., Valdimarsson, H., Jónsson, S., Torres, D. J., et al. (2011). Significant role of the North Icelandic Jet in the formation of Denmark Strait overflow water. *Nature Geoscience*, *4*(10), 723–727. https://doi.org/10.1038/ngeo1234

Vockenhuber, C., Casacuberta, N., Christl, M., & Synal, H.-A. (2015). Accelerator mass spectrometry of ^{129}I towards its lower limits. *Nuclear Instruments and Methods in Physics Research Section B: Beam Interactions with Materials and Atoms*, *361*, 445–449. https://doi.org/10.1016/j.nimb.2015.01.061

Wefing, A. (2021). *^{129}I and ^{236}U as a new tracer pair to study water mass circulation in the Arctic Ocean and Fram Strait* (p. 254). ETH Zurich. https://doi.org/10.3929/ETHZ-B-000491713

Wefing, A., Casacuberta, N., Christl, M., Gruber, N., & Smith, J. N. (2021). Circulation timescales of Atlantic Water in the Arctic Ocean determined from anthropogenic radionuclides. *Ocean Science*, *17*(1), 111–129. https://doi.org/10.5194/os-17-111-2021

Wefing, A., Christl, M., Vockenhuber, C., Rutgers van der Loeff, M., & Casacuberta, N. (2019). Tracing Atlantic Waters Using ^{129}I and ^{236}U in the Fram Strait in 2016. *Journal of Geophysical Research: Oceans*, *124*(2), 882–896. https://doi.org/10.1029/2018JC014399

Weijer, W., Haine, T., Siddiqui, A., Cheng, W., Veneziani, M., & Kurtakoti, P. (2022). Interactions between the Arctic Mediterranean and the Atlantic Meridional Overturning Circulation: A review. *Oceanography*, *35*(3–4), 118–127. https://doi.org/10.5670/oceanog.2022.130

Yashayaev, I., Bersch, M., & van Aken, H. M. (2007). Spreading of the Labrador Sea Water to the Irminger and Iceland basins. *Geophysical Research Letters*, *34*(10), 2006GL028999. https://doi.org/10.1029/2006GL028999

Yashayaev, I., & Dickson, B. (2008). Transformation and fate of overflows in the Northern North Atlantic. In R. R. Dickson, J. Meincke, & P. Rhines (Eds.), *Arctic–Subarctic ocean fluxes* (pp. 505–526). Springer. https://doi.org/10.1007/978-1-4020-6774-7_22

Zou, S., Bower, A., Furey, H., Susan Lozier, M., & Xu, X. (2020). Redrawing the Iceland−Scotland overflow water pathways in the North Atlantic. *Nature Communications*, *11*(1), 1890. https://doi.org/10.1038/s41467-020-15513-4